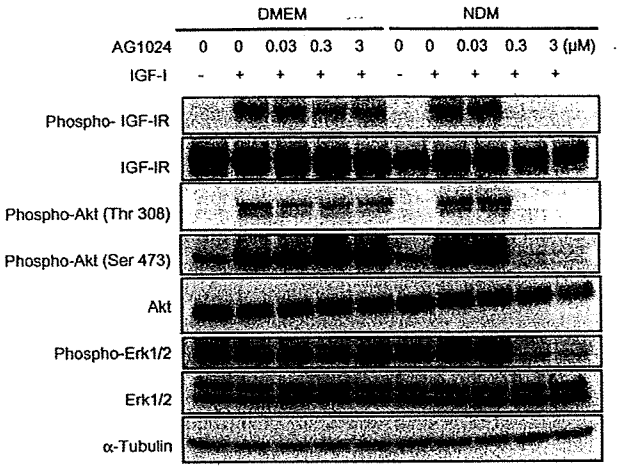

Fig. 2. Effect of AG1024 on IGF-1R activation. PANC-1 cells incubated in DMEM for 24 h were washed with PBS and the medium was replaced with either fresh DMEM or NDM. The cells were incubated with the indicated concentration of AG1024 for 1 h before stimulation with 50 ng/ml IGF-1 for 10 min. Cell lysates were resolved using SDS–PAGE and transferred to membranes for western blotting with specific antibodies.

anti-phospho-Erk, or anti-tubulin antibodies. Horseradish peroxidase-linked anti-rabbit IgG or anti-mouse IgG antibodies were used as secondary antibodies (GE Healthcare, Piscataway, NJ). The blots were developed using ECL reagent according to the manufacturer's instructions (GE healthcare).

Flow cytometric analysis. PANC-1 cells (5×10^5) in 60-mm dishes were incubated in DMEM for 24 h. The cells were washed with PBS and the medium was replaced with either fresh DMEM or NDM. AG1024 (0.3 μM) was then added and the cells were cultured for 12 h. The cells were incubated with annexin V-FITC and propidium iodide using an annexin V-FITC apoptosis detection kit (Biovision Research Products, Mountain View, CA) and analyzed using a flow cytometer (FACSCalibur; BD Biosciences, Franklin Lakes, NJ).

Statistical analysis. All data are representative of three independent experiments with similar results. The statistical data are expressed as mean ± SD using descriptive statistics.

Results

AG1024 is preferentially cytotoxic to human pancreatic cancer PANC-1 cells in nutrient-deprived conditions

To identify cytotoxic agents that function preferentially on nutrient-deprived cells, we tested the cytotoxic effects of small-molecule inhibitors in the SCADS inhibitors kit I. As shown in Table S1, a specific inhibitor of IGF-1R tyrosine kinase, termed AG1024, was found to be cytotoxic to PANC-1 cells in nutrient-deprived medium (NDM), but not in normal medium (DMEM). The structure of AG1024 [22], otherwise known as 2-(3-bromo-5-*t*-butyl-4-hydroxybenzylidene)malonitrile, is shown in Fig. 1A. To determine the dose–response relationship of AG1024 cytotoxicity, PANC-1

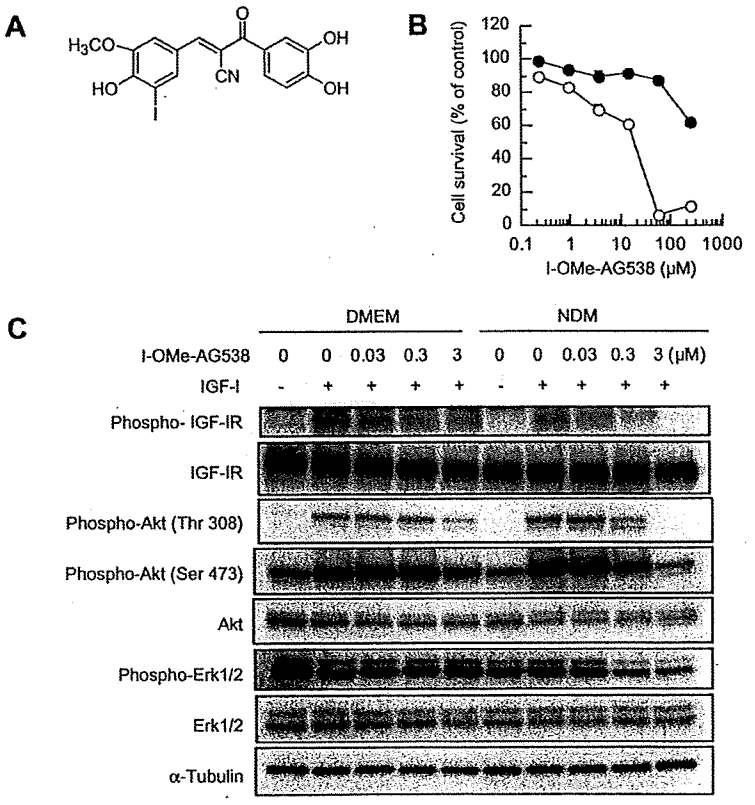

Fig. 3. Effect of I-OMe-AG538 on survival of nutrient-deprived PANC-1 cells. (A) Structure of I-OMe-AG538. (B) Effect of I-OMe-AG538 on PANC-1 cell viability in DMEM (●) or NDM (○). PANC-1 cells were incubated with the indicated concentrations of I-OMe-AG538 in DMEM or NDM for 24 h. (C) Effect of I-OMe-AG538 on IGF-1R activation. PANC-1 cells in DMEM or NDM were incubated with the indicated concentration of I-OMe-AG538 for 1 h before stimulation with 50 ng/ml IGF-1 for 10 min. Cell lysates were resolved using SDS–PAGE and transferred to membranes for western blotting with specific antibodies.

cells grown in NDM or DMEM were exposed to increasing concentrations of AG1024 for 24 h (Fig. 1B). The cytotoxic effect of AG1024 was more than 100 times greater on nutrient-deprived PANC-1 cells (NDM IC_{50} 0.055 μM) relative to cells in nutrient-sufficient medium (DMEM IC_{50} 21 μM). In DMEM, 0.3 μM AG1024 did not induce any significant PANC-1 cell death as determined using propidium iodide and annexin V staining and flow cytometry (Fig. 1C). In contrast, 34% of the cells grown in NDM and treated with the same concentration of AG1024 showed propidium iodide-positive/annexin V-negative staining. We compared the cytotoxicity of AG1024 to that of several conventional anticancer drugs, including doxorubicin, 5-fluorouracil and paclitaxel, in PANC-1 cells grown in NDM versus DMEM (Fig. 1D). The cytotoxicity of doxorubicin, 5-fluorouracil and paclitaxel on PANC-1 cells grown in either medium for 24 h was significantly weaker than AG1024. These results demonstrate clearly that AG1024 exhibits preferential cytotoxicity to nutrient-deprived PANC-1 cells.

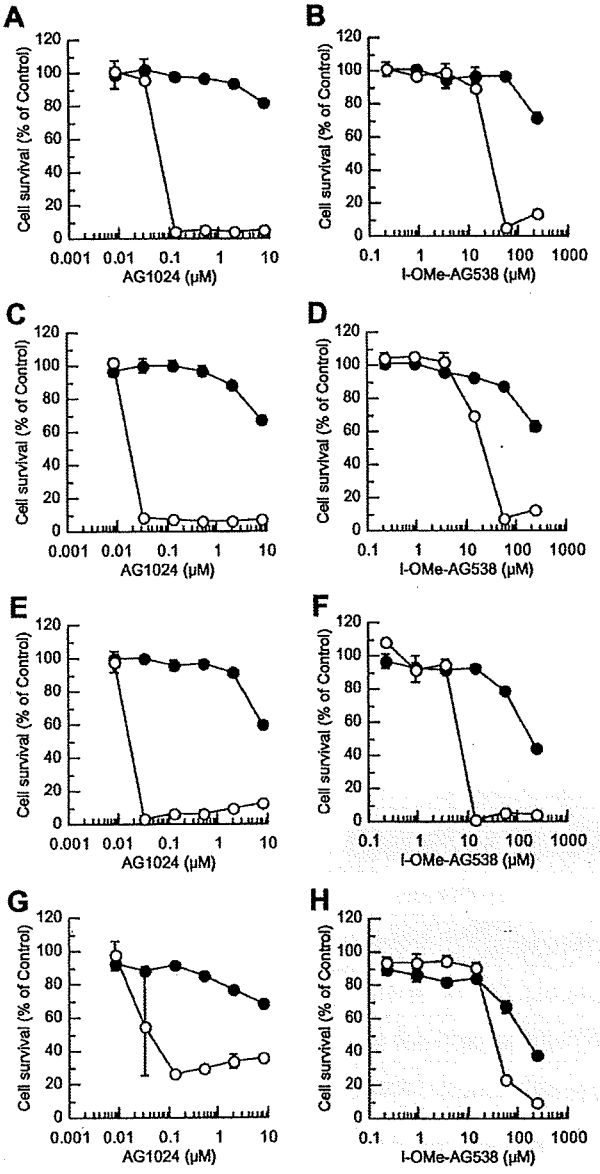

Fig. 4. Effect of AG1024 and I-OMe-AG538 on various human pancreatic cancer cell lines in nutrient-deprived conditions. Human pancreatic cancer cells were incubated with indicated concentrations of AG1024 or I-OMe-AG538 in DMEM (●) or NDM (○) for 24 h. A,B, Capan-1; C,D, MIA Paca-2; E,F, BxPC-3; G,H, PSN-1.

AG1024 inhibits activation of IGF-1R in nutrient-deprived PANC-1 cells

Because AG1024 is a specific inhibitor of IGF-1R kinase, we examined the effect of AG1024 on IGF-1-mediated phosphorylation of IGF-1R in PANC-1 cells grown in different media (Fig. 2). While addition of 0.3 μM AG1024 to PANC-1 cells grown in NDM resulted in a complete inhibition of IGF-1R autophosphorylation, phosphorylation of IGF-1R was only weakly inhibited in cells grown in DMEM with 10-fold higher concentrations of AG1024 (3 μM). AG1024 also inhibited the phosphorylation of Akt (Thr 308), Akt (Ser 473) and Erk, which normally occur as a result of IGF-1R activation. These results demonstrate that AG1024 is a potent inhibitor of IGF-1R activation in nutrient-deprived PANC-1 cells.

I-OMe-AG538 is preferentially cytotoxic to nutrient-deprived PANC-1 cells

In testing whether other IGF-1R inhibitors also functioned preferentially in nutrient-deprived cells, we found that I-OMe-AG538 [23] (another specific inhibitor of IGF-1R, Fig. 3A) also was more cytotoxic to cells in nutrient-deprived medium relative to those in nutrient-sufficient conditions (Fig. 3B). The effect of I-OMe-AG538 on IGF-1R activation in nutrient-deprived cells was similar to AG1024, in that it blocked phosphorylation of IGF-1R, Akt and Erk (Fig. 3C). Our results demonstrate clearly that the IGF-1R inhibitors AG1024 and I-OMe-AG538 both inhibit IGF-1R-mediated signaling and are preferentially cytotoxic to nutrient-deprived PANC-1 cells.

Inhibitors of IGF-1R show preferential cytotoxicity to various human pancreatic cancer cells lines in nutrient-deprived conditions

To determine whether inhibitors of IGF-1R kinase exhibit preferential cytotoxicity to other nutrient-deprived human pancreatic cancer cell lines, we examined the cytotoxic effects of AG1024 and I-OMe-AG538 on Capan-1, MIA Paca-2, BxPC-3, and PSN cells (Fig. 4). AG1024 and I-OMe-AG538 were significantly more cytotoxic to all four human pancreatic cancer cell lines in NDM relative to DMEM, indicating that the cytotoxicity of IGF-1R kinase inhibitors is likely to occur in nutrient-deprived human pancreatic cancer cells. To understand the specificity of IGF-1R kinase inhibitors, we also examined the cytotoxic effects of other representative receptor tyrosine kinase inhibitors (Fig. S1). The cytotoxicities of AG1296 (a PDGFR kinase inhibitor) [24] and AG1478 and PD168393 (EGFR kinase inhibitors) [25–27] were significantly reduced, relative to IGF-1R inhibitors, in both nutrient-deprived and -fed PANC-1 cells. These results indicate that specific inhibition of IGF-1R kinase is important in promoting preferential cytotoxicity in nutrient-starved human pancreatic cancer cells.

Discussion

Tumor microenvironment strongly influences tumor growth and progression. Many aspects of physiology that differentiate solid tumors from normal tissues arise from differences in vasculature. Disorganized vascular systems in tumors result in large areas of tumor exposed to nutrient starvation and hypoxic conditions. In addition, due to the unregulated growth of tumor cells caused by genetic and epigenetic alterations, cells proliferate more rapidly than normal cells and nutrient and oxygen demands often exceeds supply [28–30]. Cancer cells, in particular highly aggres-

sive tumors such as pancreatic cancer that are relatively hypovascular, are able to survive even in conditions of low nutrients and low oxygen supply. Since chronic nutrient deprivation seldom occurs in normal tissues, one strategy for anticancer agent development is to target cancer cells growing in nutrient-deprived conditions. Thus, we screened to identify cytotoxic agents that function preferentially in nutrient-deprived cells.

We found that AG1024, a specific inhibitor of IGF-1R kinase, showed preferential cytotoxicity to human pancreatic cancer PANC-1 cells grown in nutrient-deprived medium. Conventional chemotherapeutic drugs such as doxorubicin, 5-fluorouracil and paclitaxel, were only weakly cytotoxic to nutrient-deprived PANC-1 cells, suggesting that AG1024 may be a unique and attractive starting compound in the development of an antitumor agent. AG1024 has been reported to induce apoptosis in human breast cancer MCF-7 cells [31]. In our present study, flow cytometric analysis showed that AG1024 increased propidium iodide staining without annexin V of nutrient-deprived PANC-1 cells. Kigamicin D and (6a*R*,11a*R*)-3,8-dihydroxy-9-methoxypterocarpan induced necrosis in nutrient-deprived cells [4,32]. Therefore, AG1024 may induce necrosis under nutrient starvation. I-OMe-AG538, another IGF-1R kinase inhibitor that differs in structure from AG1024, was also cytotoxic to nutrient-deprived PANC-1 cells. These IGF-1R kinase inhibitors also were cytotoxic to other nutrient-deprived human pancreatic cancer cell lines, including Capan-1, MIA Paca-2, BxPC-3 and PSN.

IGF-1 binding to the IGF-1R results in activation of receptor tyrosine kinases that stimulates signaling through intracellular networks, including PI3K-AKT-TOR and RAF-MAPK, which then promote cell proliferation and inhibit apoptosis. We found that the IGF-1R kinase inhibitors AG1024 and I-OMe-AG538 blocked phosphorylation of IGF-1R by IGF-1 preferentially in cells cultured in nutrient-deprived conditions relative to those in nutrient-sufficient conditions. These IGF-1R kinase inhibitors also suppressed phosphorylation of Akt and Erk, demonstrating that activation of pathways downstream of the IGF-1R were also blocked in nutrient-deprived conditions.

Unlike AG1296 (a PDGFR kinase inhibitor) or AG1478 and PD168393 (EGFR kinase inhibitors), which are less cytotoxic in nutrient-deprived PANC-1 cells, preferential inhibition of IGF-1 signaling by IGF-1R kinase inhibitors suggests that this pathway may play an important role in cell survival in stress conditions such as nutrient deprivation. The Akt pathway, which functions downstream of IGF-1R, plays a critical role in the proliferation, survival, motility, morphology and therapeutic resistance of cancer cells [33,34]. Because Akt has been demonstrated to regulate cell survival in various stress conditions, including nutrient deprivation, this kinase is viewed as a promising target for cancer therapeutics. Akt inhibitors have been developed including PX-316, which shows antitumor activity against human MCF-7 breast cancer and HT-29 colon cancer xenografts in mice [35]. Thus, part of the preferential cytotoxicity of IGF-1R kinase inhibitors in nutrient-deprived conditions may be due to inhibition of Akt activation.

The IGF-1 receptor is universally expressed in various hematologic and solid tumor cells. NVP-ADW742, another specific inhibitor of IGF-1R kinase, has been shown to be a significant antitumor agent in an orthotopic xenograft multiple myeloma model [20]. Oral administration of the IGF-1R kinase-specific inhibitor NVP-AEW541 has been shown to inhibit IGF-1R signaling in tumors and to reduce tumor growth in a xenograft fibrosarcoma model [19]. The potent cytotoxicity of AG1024 and I-OMe-AG538 to pancreatic cancer cell lines deprived of nutrients (simulating a tumor microenvironment) makes IGF-1R a promising target for new drugs that may be developed to treat a broad spectrum of malignant tumors.

Acknowledgments

This work was supported by Grant-in-Aid for the Third-Term Comprehensive 10-Years Strategy for Cancer Control from the Ministry of Health, Labour and Welfare in Japan. We thanks Dr. H. Esumi (National Cancer Center Hospital East, Japan) for helpful advice, Ms. S. Kakuda for technical assistance and Screening Committee of Anticancer Drugs supported by Grant-in-Aid for Scientific Research on Priority Area "Cancer" from the Ministry of Education, Culture, Sports, Science and Technology, Japan for supplying the SCADS inhibitor kit I.

Appendix A. Supplementary data

Supplementary data associated with this article can be found, in the online version, at doi:10.1016/j.bbrc.2009.01.065.

References

[1] D. Li, K. Xie, R. Wolff, J.L. Abbruzzese, Pancreatic cancer, Lancet 363 (2004) 1049–1057.
[2] S. Shore, D. Vimalachandran, M.G. Raraty, P. Ghaneh, Cancer in the elderly: pancreatic cancer, Surg. Oncol. 13 (2004) 201–210.
[3] K. Izuishi, K. Kato, T. Ogura, T. Kinoshita, H. Esumi, Remarkable tolerance of tumor cells to nutrient deprivation: possible new biochemical target for cancer therapy, Cancer Res. 60 (2000) 6201–6207.
[4] J. Lu, S. Kunimoto, Y. Yamazaki, M. Kaminishi, H. Esumi, D. Kigamicin, A novel anticancer agent based on a new anti-austerity strategy targeting cancer cells' tolerance to nutrient starvation, Cancer Sci. 95 (2004) 547–552.
[5] S. Kunimoto, J. Lu, H. Esumi, Y. Yamazaki, N. Kinoshita, Y. Honma, M. Hamada, M. Ohsono, M. Ishizuka, T. Takeuchi, D. Kigamicins, Novel antitumor antibiotics. I. Taxonomy, isolation, physico-chemical properties and biological activities, J. Antibiot. 56 (2003) 1004–1011.
[6] S. Kunimoto, T. Someno, Y. Yamazaki, J. Lu, H. Esumi, H. Naganawa, D. Kigamicins, Novel antitumor antibiotics. II. Structure determination, J. Antibiot. 56 (2003) 1007–1012.
[7] H. Esumi, J. Lu, Y. Kurashima, T. Hanaoka, Antitumor activity of pyrvinium pamoate, 6-(dimethylamino)-2-[2-(2,5-dimethyl-1-phenyl-1H-pyrrol-3-yl)ethenyl]-1-methyl-quinolinium pamoate salt, showing preferential cytotoxicity during glucose starvation, Cancer Sci. 95 (2004) 685–690.
[8] M.N. Pollak, E.S. Schernhammer, S.E. Hankinson, Insulin-like growth factors and neoplasia, Nat. Rev. Cancer 4 (2004) 505–518.
[9] A. Ullricha, J. Schlessingerb, Signal transduction by receptors with tyrosine kinase activity, Cell 61 (1990) 203–212.
[10] P.V.D. Geer, T. Hunter, R.A. Lindberg, Receptor protein-tyrosine kinases and their signal transduction pathways, Annu. Rev. Cell Biol. 10 (1994) 251–337.
[11] R. Baserga, The contradictions of the insulin-like growth factor 1 receptor, Oncogene 19 (2000) 5574–5581.
[12] E.A. Bohula, A.J. Salisbury, M. Sohail, M.P. Playford, J. Riedemann, E.M. Southern, V.M. Macaulay, The efficacy of small interfering RNAs targeted to the type 1 insulin-like growth factor receptor (IGF1R) is influenced by secondary structure in the IGF1R transcript, J. Biol. Chem. 278 (2003) 15991–15997.
[13] E.K. Maloney, J.L. McLaughlin, N.E. Dagdigian, L.M. Garrett, K.M. Connors, X.-M. Zhou, W.A. Blättler, T. Chittenden, R. Singh, An anti-insulin-like growth factor I receptor antibody that is a potent inhibitor of cancer cell proliferation, Cancer Res. 63 (2003) 5073–5083.
[14] D. Burtrum, Z. Zhu, D. Lu, D.M. Anderson, M. Prewett, D.S. Pereira, R. Bassi, R. Abdullah, A.T. Hooper, H. Koo, X. Jimenez, D. Johnson, R. Apblett, P. Kussie, P. Bohlen, L. Witte, D.J. Hicklin, D.L. Ludwig, A fully human monoclonal antibody to the insulin-like growth factor I receptor blocks ligand-dependent signaling and inhibits human tumor growth in vivo, Cancer Res. 63 (2003) 8912–8921.
[15] P. Hayry, M. Myllarniemi, E. Aavik, S. Alatalo, P. Aho, S. Yilmaz, A.R. Sokolowski, G. Cozzone, B. Jameson, R. Baserga, Stabile D-peptide analog of insulin-like growth factor-1 inhibits smooth muscle cell proliferation after carotid ballooning injury in the rat, FASEB J. 9 (1995) 1336–1344.
[16] D. Sachdev, J.S. Hartell, A.V. Lee, X. Zhang, D. Yee, A dominant negative type I insulin-like growth factor receptor inhibits metastasis of human cancer cells, J. Biol. Chem. 279 (2004) 5017–5024.
[17] C.-T. Lee, K.-H. Park, Y. Adachi, J.Y. Seol, C.-G. Yoo, Y.W. Kim, S.K. Han, Y.-S. Shim, K. Coffee, M.M. Dikov, D.P. Carbone, Recombinant adenoviruses expressing dominant negative insulin-like growth factor-I receptor demonstrate antitumor effects on lung cancer, Cancer Gene. Ther. 10 (2003) 57–63.
[18] Y. Min, Y. Adachi, H. Yamamoto, H. Ito, F. Itoh, C.-T. Lee, S. Nadaf, D.P. Carbone, K. Imai, Genetic blockade of the insulin-like growth factor-I receptor: a promising strategy for human pancreatic cancer, Cancer Res. 63 (2003) 6432–6441.
[19] C. García-Echeverría, M.A. Pearson, A. Marti, T. Meyer, J. Mestan, J. Zimmermann, J. Gao, J. Brueggen, H.-G. Capraro, R. Cozens, D.B. Evans, D.

Fabbro, P. Furet, D.G. Porta, J. Liebetanz, G. Martiny-Baron, S. Ruetz, F. Hofmann, In vivo antitumor activity of NVP-AEW541—a novel, potent, and selective inhibitor of the IGF-IR kinase, Cancer Cell 5 (2004) 231–239.
[20] C.S. Mitsiades, N.S. Mitsiades, C.J. McMullan, V. Poulaki, R. Shringarpure, M. Akiyama, T. Hideshima, D. Chauhan, M. Joseph, T.A. Libermann, C. García-Echeverría, M.A. Pearson, F. Hofmann, K.C. Anderson, Andrew L. Kung, Inhibition of the insulin-like growth factor receptor-1 tyrosine kinase activity as a therapeutic strategy for multiple myeloma, other hematologic malignancies, and solid tumors, Cancer Cell 5 (2004) 221–230.
[21] T. Mosmann, Rapid colorimetric assay for cellular growth and survival: application to proliferation and cytotoxicity assays, J. Immunol. Methods 65 (1983) 55–63.
[22] B. Wen, E. Deutsch, E. Marngoni, V. Frascona, L. Maggiorella, B. Abdulkarim, N. Chavaudra, J. Bourhis, Tyrphostin AG 1024 modulates rediosensitivity in human breast cancer cells, Br. J. Cancer 85 (2001) 2017–2021.
[23] G. Blum, A. Gazit, A. Levitzki, Substrate competitive inhibitors of IGF-1 receptor kinase, Biochemistry 39 (2000) 15705–15712.
[24] L.M. Strawn, G. McMahon, H. App, R. Schreck, W.R. Kuchler, M.P. Longhi, T.H. Hui, C. Tang, A. Levitzki, A. Gazit, I. Chen, G. Keri, L. Orfi, W. Risau, I. Flamme, A. Ullrich, K.P. Hirth, L.K. Shawver, Flk-1 as a target for tumor growth inhibition, Cancer Res. 56 (1996) 3540–3545.
[25] A. Levitzki, A. Gazit, Tyrosine kinase inhibition: an approach to drug development, Science 267 (1995) 1782–1788.
[26] R. Bose, H. Molina, A.S. Patterson, J.K. Bitok, B. Periaswamy, J.S. Bader, A. Pandey, P.A. Cole, Phosphoproteomic analysis of Her2/neu signaling and inhibition, Proc. Natl. Acad. Sci. USA 103 (2006) 9773–9778.
[27] D.W. Fry, A.J. Bridges, W.A. Denny, A. Doherty, K.D. Greis, J.L. Hicks, K.E. Hook, P.R. Keller, W.R. Leopold, J.A. Loo, D.J. McNamara, J.M. Nelson, V. Sherwood, J.B. Smaill, S. Trumpp-Kallmeyer, E.M. Dobrusin, Specific, irreversible inactivation of the epidermal growth factor receptor and erbB2, by a new class of tyrosine kinase inhibitor, Proc. Natl. Acad. Sci. USA 95 (1998) 12022–12027.
[28] C.V. Dang, G.L. Semenza, Oncogenic alterations of metabolism, Trends Biochem. Sci. 24 (1999) 68–72.
[29] R.M. Southerland, Cell and environment interactions in tumor microregions: the multicell spheroid model, Science 240 (1988) 178–184.
[30] G. Helmlinger, F. Yuan, M. Dellian, R.K. Jain, Interstitial pH and pO_2 gradients in solid tumors in vivo: high-resolution measurements reveal a lack of correlation, Nat. Med. 3 (1997) 177–182.
[31] P. Marcelina, G. Aviv, L. Alexander, W. Efrat, L. Derek, Specific inhibitor of insulin-like growth factor-1 and insulin receptor tyrosine kinase activity and biological function by tyrphostins, Endocrinology 138 (1997) 1427–1433.
[32] S. Awale, F. Li, H. Onozuka, H. Esumi, Y. Tezuka, S. Kadota, Constituents of Brazilian red propolis and their preferential cytotoxic activity against human pancreatic PANC-1 cancer cell line in nutrient-deprived condition, Bioorg. Med. Chem. 16 (2008) 181–189.
[33] A. Toker, M. Yoeli-Lerner, Akt signaling and cancer: surviving but not moving on, Cancer Res. 66 (2006) 3963–3966.
[34] A.G. Bader, S. Kang, L. Zhao, P.K. Vogt, Oncogenic PI3K deregulates transcription and translation, Nat. Rev. Cancer 5 (2005) 921–929.
[35] E.J. Meuillet, N. Ihle, A.F. Baker, J.M. Gard, C. Stamper, R. Williams, A. Coon, D. Mahadevan, B.L. George, L. Kirkpatrick, G. Powis, In vivo molecular pharmacology and antitumor activity of the targeted Akt inhibitor PX-316, Oncol. Res. 14 (2004) 513–527.

Autophagy is activated in pancreatic cancer cells and correlates with poor patient outcome

Satoshi Fujii,[1] Shuichi Mitsunaga,[2] Manabu Yamazaki,[1] Takahiro Hasebe,[3] Genichiro Ishii,[1] Motohiro Kojima,[1] Taira Kinoshita,[4] Takashi Ueno,[5] Hiroyasu Esumi[6] and Atsushi Ochiai[1,7]

[1]Pathology Division, Research Center for Innovative Oncology, National Cancer Center Hospital East, 6-5-1 Kashiwanoha, Kashiwa, Chiba 277-8577; [2]Division of Hepatobiliary and Pancreatic Oncology, National Cancer Center Hospital East, 6-5-1 Kashiwanoha, Kashiwa, Chiba 277-8577; [3]Office for Pathology Consultation and Service, Clinical Trials and Practice Support Division, Center for Cancer Control and Information Services, National Cancer Center, 5-1-1, Tsukiji, Chuo-ku, Tokyo 104-0045; [4]Department of Hepatobiliary-Pancreatic Surgery, National Cancer Center Hospital East, 6-5-1 Kashiwanoha, Kashiwa, Chiba, 277-8577; [5]Department of Biochemistry, Juntendo University School of Medicine, 2-1-1 Hongo, Bunkyo-ku, Tokyo 113-8421; [6]Cancer Physiology Project, Research Center for Innovative Oncology, National Cancer Center Hospital East, 6-5-1 Kashiwanoha, Kashiwa, Chiba 277-8577, Japan

(Received April 5, 2008/Revised May 24, 2008/Accepted May 27, 2008/Online publication July 4, 2008)

Because autonomous proliferating cancer cells are often exposed to hypoxic conditions, there must be an alternative metabolic pathway, such as autophagy, that allows them to obtain energy when both oxygen and glucose are depleted. We previously reported finding that autophagy actually contributes to cancer cell survival in colorectal cancers both *in vitro* and *in vivo*. Pancreatic cancer remains a devastating and poorly understood malignancy, and hypoxia in pancreatic cancers is known to increase their malignant potential. In the present study archival pancreatic cancer tissue was retrieved from 71 cases treated by curative pancreaticoduodenectomy. Autophagy was evaluated by immunohistochemical staining with anti-LC3 antibody, as LC3 is a key component of autophagy and has been used as a marker of autophagy. The results showed that strong LC3 expression in the peripheral area of pancreatic cancer tissue was correlated with a poor outcome ($P = 0.0170$) and short disease-free period ($P = 0.0118$). Two of the most significant correlations among the clinicopathological factors tested were found between the peripheral intensity level of LC3 expression and tumor size ($P = 0.0098$) or tumor necrosis ($P = 0.0127$). Activated autophagy is associated with pancreatic cancer cells, and autophagy is thought to be a response to factors in the cancer microenvironment, such as hypoxia and poor nutrient supply. This is the first study to report the clinicopathological significance of autophagy in pancreatic cancer. (*Cancer Sci* 2008; 99: 1813–1819)

Cancers are abnormal tissue masses whose growth exceeds and is uncoordinated with that of adjacent normal tissues, and which persist in the same excessive manner after cessation of the stimulus that evoked them.[1] All cancers ultimately depend on the host for their nutrition and blood supply, but as the preexisting vasculature is obviously insufficient to support the cancers' unlimited requirements for energy and nutrition as a result of their unregulated growth, angiogenesis has been considered pivotal to providing proliferating cancer cells with an adequate source of oxygen, energy, and nutrients. However, recent studies have revealed that even after new blood vessels have formed, both the oxygen and glucose supply is insufficient for the aggressively proliferating cancer cells in locally advanced cancers.[2–4] Tumor hypoxia has been used as a marker of poor prognosis;[5,6] however, how cancer cells become more malignant or survive with an extremely poor blood supply, as for example in pancreatic cancer, is poorly understood.[7] When cancer cells are exposed to hypoxia, anaerobic glycolysis increases and provides energy for cell survival, but as the glucose supply is also insufficient because of the poor blood supply, there must be an alternative metabolic pathway that provides energy when both oxygen and glucose are depleted.[8,9] We have reported that several cancer cell lines, including pancreatic cancer- and colorectal cancer-derived cell lines, are resistant to nutrient-deprived conditions. We have named this starvation-resistant phenotype 'austerity' and speculated that austerity may contribute to cancer cell survival in a nutrient-deficient microenvironment.[8,9]

Autophagy has long been known to be a non-specific self-degradation mechanism that is triggered by nutrient deprivation, but recently it has been shown to play an important role in removing redundant or faulty cell components, such as damaged mitochondria and other organelles that are targeted for lysosomal degradation.[10] The autophagic process occurs in three steps: (1) autophagosome formation; (2) lysosomal fusion with the autophagosome; and (3) lysosomal degradation. In step 1, a cup-shaped lipid bilayer called the isolation membrane is formed and engulfs cytosolic components, including organelles. In step 2, the isolation membrane closes, forming an autophagosome. Cytosolic LC3 (microtubule-associated protein 1 light chain 3), a mammalian homolog of yeast ATG8, is converted to LC3-I (soluble unlipidated form of LC3) during this step and LC3-I is then modified to form LC-3-II (a membrane-bound form) and becomes localized on autophagosomes. Autophagosomes fuse with lysosomes to form autolysosomes. In step 3, the contents of the autolysosomes are degraded rapidly by lysosomal hydrolases, including cathepsins B, D, and L. Intra-autophagosomal LC3-II is also degraded at the same time.[11] Thus, LC3 is a key component of autophagy, and it has been used as a marker of autophagy.

Pancreatic cancer remains a devastating and poorly understood malignancy. Its poor prognosis has been attributed to the inability to make a diagnosis while the tumor is still resectable and a propensity toward early vascular dissemination and spread to regional lymph nodes. Up to 60% of patients have advanced pancreatic cancer at the time of diagnosis, and their median survival time is a dismal 3–6 months.[12] Several pathological features, including tumor size, tumor grade, nodal metastasis, lymphatic or vascular infiltration, and perineural invasion, have been reported to be prognostic pathological parameters for patients with invasive ductal carcinoma (IDC) of the pancreas.[13–20] However, their prognostic value has been a matter of controversy because the studies were based on relatively small numbers of IDC patients. Hypoxia in pancreatic cancer has been reported to increase its malignant potential.[5,6] Studies investigating associations between tumor necrosis in IDC and expression of hypoxic markers, such as hypoxia-inducible factor-1α or carbonic anhydrase IX (CA IX), are expected to provide useful information concerning hypoxia-driven angiogenesis in IDC of the pancreas.[21–23] However, most tissue samples of IDC of the pancreas have been found to be relatively hypovascular compared with the surrounding pancreatic tissue.[7] Proliferating cancer cells require more nutrients

[7]To whom correspondence should be addressed. E-mail: aochiai@east.ncc.go.jp

doi: 10.1111/j.1349-7006.2008.00893.x

than surrounding non-cancerous cells do, though nutrition is supplied via functionally structurally immature neovessels. In other words, because autonomous proliferating cancer cells are often exposed to hypoxic conditions, autophagy is a marker of malignant transformation under hypoxic stress. We speculate that the important process for cancer cells might be autophagy as hypoxia in pancreatic cancer has been reported to be a marker of poor prognosis.[5,6]

Experimental evidence supports a role for autophagy in both cancer development and suppression. Because autophagy-specific genes promote the survival of normal cells during nutrient starvation in all eukaryotic organisms, autophagy may support the survival of rapidly growing cancer cells that have outgrown their vascular supply and are exposed to an inadequate oxygen supply or metabolic stress. By contrast, excessive levels of autophagy promote cell death, presumably via self-cannibalization. Antitumor effects are observed at all levels of autophagy, in the form of either cell death (when the autophagy level is very low or very high) or cell death-independent tumor-suppressor effects (when the autophagy level is intermediate).[24] There might be a balance between the autophagy level and survival of rapidly growing cancer cells if autophagy were turned on or off, according to the nutritional status of cancer cells during the processes of growth, invasion, and metastasis. In a previous study, we showed that autophagosomes are produced actively and consumed promptly in colorectal cancer cells during amino acid starvation, and autophagosome formation was seen only in the tumor cells, never in the adjacent non-cancerous cells. In other words, we found that active autophagy contributes to cancer cell survival in colorectal cancers both *in vitro* and *in vivo*.[25]

It is easy to speculate that the pathophysiological role of autophagy in proliferating cancer cells varies with the type of cancer cell. Autophagy is thought to react to the cancer microenvironment, such as hypoxia and low nutrient supply. There have been no reports of studies on how autophagy functions in cancer tissue, comprising cancer cells and their microenvironment. In the present study we extended our investigation to an *in vivo* study of pancreatic cancer tissue and to elucidating the significance of autophagy in cancer tissue.

Materials and Methods

Patients. The subjects of this study were 71 patients who underwent curative pancreaticoduodenectomy at the National Cancer Center Hospital East, Chiba, Japan between December 1992 and February 2004. The pathological diagnosis in every case was IDC of the pancreas. The median age of the patients was 65 years (mean age 64.3 years), and 31 patients were women. None of the patients received neo-adjuvant therapy before the operation. Regional lymph node dissection was carried out in all patients. None of the 71 patients received adjuvant therapy. All patients agreed to enrollment in the study and each gave informed consent. The institutional review board of the National Cancer Center approved all protocols on the patients' agreements.

Pathological examination. The resected specimens were fixed in 10% formalin at room temperature, and the size and gross appearance of the tumors were recorded. The entire tumor was sectioned at intervals of approximately 0.5 cm, and all tumor-containing sections were processed routinely and embedded in paraffin. Serial sections of each tumor were cut and stained with hematoxylin–eosin, and then examined to confirm the pathological diagnosis. Elastica staining was used to examine them for blood vessel infiltration.

Clinicopathological parameters. The prognostic value of the following histological parameters was assessed in the present study: (1) age (≥65 vs <65 years); (2) sex; (3) tumor size (≥3 vs <3 cm); (4) predominant differentiation of the tumor (well, moderately, or poorly differentiated); (5) lowest degree of tumor differentiation (well, moderately, or poorly differentiated); (6) lymphatic vessel infiltration (≥2 [score 2 or 3] vs <2 [score 0 or 1]); (7) blood vessel infiltration (≥2 [score 2 or 3] vs <2 [score 0 or 1]); (8) intrapancreatic neural invasion (≥2 [score 2 or 3] vs <2 [score 0 or 1]); (9) retroperitoneal invasion (absent vs present); (10) International Union Against Cancer (UICC) pathological T (pT) category (pT1, pT2, or pT3); (11) UICC pathological N (pN) category (pN0 vs pN1); (12) UICC pathological stage (pStage) (≥pStageIIB vs ≤pStageIIA); (13) tumor necrosis (absent vs present); and (14) nerve plexus invasion (absent vs present).[26] Fourteen histological parameters were evaluated in this study according to the UICC,[26] World Health Organization,[27] and the Japan Pancreas Society.[28] Predominant and lowest differentiation was evaluated according to the World Health Organization classification.[27] Tumor necrosis was defined as confluent cell death in invasive areas of primary cancers, visible at an objective lens magnification of ×4.[20]

Outcome. All 71 patients were followed for survival, and the follow-up period was measured from the date of surgery to 29 November 2004. The median follow-up period was 371 days. Overall, 34 patients were diagnosed with local recurrence, 31 patients with liver metastasis, and nine patients with peritoneal metastasis during the follow-up period. Fifty-eight patients died of their disease. Recurrence was defined as initial tumor recurrence. Metastasis or local recurrence was considered as evidence of tumor relapse, and only deaths from pancreatic cancer were considered for the purposes of this study.

Immunohistochemical staining. The method of production of rabbit polyclonal LC3 antibody and of immunohistochemical staining for LC3 have been described previously.[25,29] Formalin-fixed, paraffin-embedded tissue sections containing the maximal cancer tissue area were processed for immunohistochemical staining to enable evaluation of the several clinicopathological factors described below. Some representative cases were used for immunohistochemical staining using rabbit polyclonal CA IX antibody (1 : 50 dilution) (H-120; sc-25599; Santa Cruz Biotechnology) as a hypoxia marker,[21] to examine whether the tumor cells with enhanced LC3 expression were under hypoxic stress.

Evaluation of LC3 expression level by immunohistochemical staining using LC3 antibody. Because nerve cells stain positive for LC3 immunohistochemically,[25] we used the immunohistochemical staining of nerve cells in the tissue as an internal positive control to validate the immunohistochemical staining in each case. Cancer cells whose staining intensity was equal to or stronger than that of nerve cells were judged to be strongly positive, whereas those whose staining was clearly weaker than that of the nerve cells were judged to be weakly positive. Cancer cells that did not stain positively for LC3 immunohistochemically despite a positive internal control were judged to be negative. We selected sections containing the maximal cancer tissue area that included the center of the cancer tissue and the periphery and invasive border between the cancer tissue and non-cancerous tissue. The midpoint between the margin and the center of the cancer tissue was defined as the border between the 'peripheral area' or 'central area'. In other words, the area outside the border and the area inside the border were defined as the peripheral area or the central area, respectively. Thus, the peripheral area contained the invasive border of cancer tissue. Figure 1 shows a schema of how the central area and the peripheral area were defined for each tumor.

The dominant intensity level of LC3-positive cells was evaluated in each central area and peripheral area as follows. The level of intensity of LC3 staining in each area was determined by the percentage of cells that stained negative, weakly positive, and strongly positive. When more than 50% of the LC3-positive cancer cells were strongly positive for LC3 in each area (peripheral area and central area), the area was evaluated as strongly positive, and when more than 50% of the LC3-positive cancer cells were weakly positive for LC3, the area was designated weakly positive.

doi: 10.1111/j.1349-7006.2008.00893.x

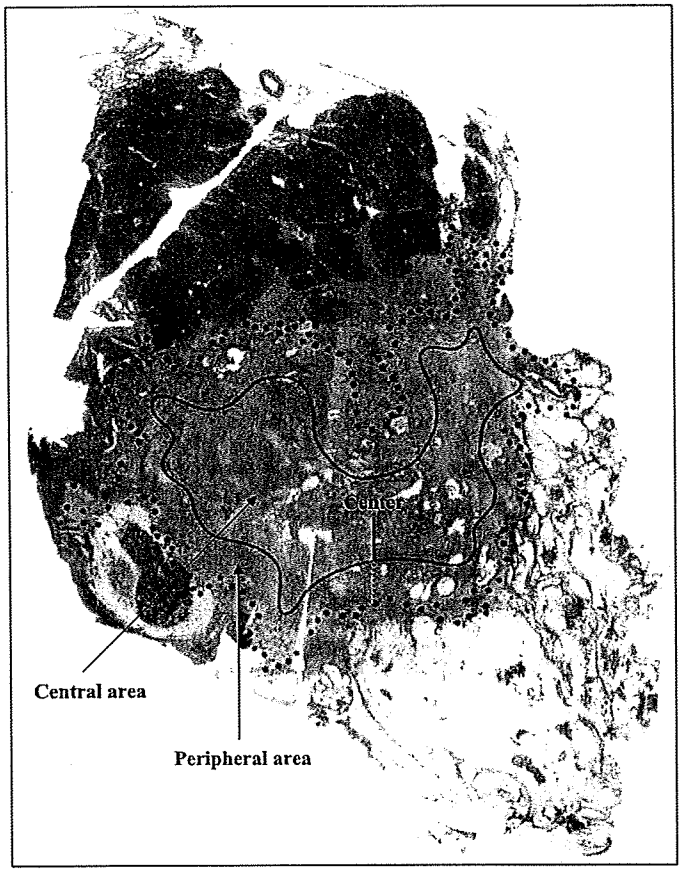

Fig. 1. The central area and the peripheral area of the pancreatic cancer tissue. We mapped the margin of the tumor tissue area of each case and drew a bold dotted line surrounding the tumor tissue area using some slides covering the entire tumor tissue. The margin of tumor tissue is shown as the bold dotted line. The center is decided from the overview. The midpoint between the margin and the center of the cancer tissue was defined as the border between the 'peripheral area' or 'central area'. As shown, the diameter (a small-dotted straight black line) from the marginal bold dotted line of the tumor tissue to the border line and the diameter (a black straight line) from the border line to the center of the tumor tissue were the same. The border line (a black curved line) was drawn so that the diameters were almost the same inside the tumor tissue area. In other words, the area outside the border and the area inside the border were defined as the 'peripheral area' and the 'central area', respectively. Thus, the peripheral area contained the invasive border of cancer tissue.

The cases were classified into three groups according to the dominant overall intensity of the cancer tissue: negative, weakly positive, or strongly positive. The dominant overall intensity in each case was determined according to the predominant intensity of LC3 positivity. When 30% of the cancer cells were weakly positive and 40% were strongly positive, the predominant intensity was recorded as strongly positive. One pathologist (S.F.) evaluated all of the immunohistochemical slides in the present study, and other pathologists (M.Y. and A.O.) also evaluated them to validate the reproducibility of immunohistochemical analyses.

The LC3 immunohistochemical staining factors were analyzed statistically to examine the relationship between clinicopathological factors, overall survival, and disease-free survival.

Statistical analysis. All methods of statistical analysis have been described in a previous report.[20] Overall survival curves and disease-free survival curves were drawn using the Kaplan–Meier method. During the overall survival and disease-free survival periods, significant differences in the levels of LC3 expression that were classified into two or three categories were examined using the log-rank test. In the present study, the clinicopathological factors of pancreatic cancer were classified into two groups similar to the previous study.[20] The relationships between the level of LC3 expression and clinicopathological factors were examined using the χ^2-test. The clinicopathological factors that were significantly associated with the expression level of LC3 in the peripheral area were further analyzed together in multivariate analyses using the Cox proportional hazard regression model to identify the factors that were most significantly associated with the tumor progression of pancreatic cancer. The *P*-values were two-sided, and the significance level was set at $P < 0.05$. All analyses were carried out using the Statview-J 5.0 package, Windows version (SAS).

Results

LC3 is expressed in pancreatic cancer tissue. As imaging analyses of pancreatic cancer *in vivo* have shown that cancer tissue is more hypovascular than the surrounding non-cancerous tissue,[7] it is speculated that cancer cells use autophagy as a means of nutrition. We evaluated autophagy in surgically resected pancreatic cancer tissue by immunohistochemical staining with anti-LC3 antibody. Formalin-fixed and paraffin-embedded tissue samples from 71 cases of IDC were processed for immunohistochemical analysis, and LC3 expression in the cancer tissue was assessed by comparing it with the staining intensity of nerve cells in intra- or peripancreatic tissue, which expresses LC3 consistently (Figs 2,3). Most pancreatic cancer tissues stained positively for LC3. Weakly or strongly positive expression of LC3 was observed in 62 of the 71 cases of IDC of the pancreas, but there were no positive cells in the cancer tissue from the other nine cases. Table 1 compares the intensity of LC3 expression between the peripheral area and central area of the pancreatic cancer tissue. Intensity in the peripheral area was negative, weakly positive, and strongly positive in nine cases (12.7%), 23 cases (32.4%) and 39 cases (54.9%), respectively. The peripheral area of the pancreatic cancer tissue was strongly positive for LC3 expression in more than half of the cases examined in the present study. The intensity in the central area was negative, weakly positive, and strongly positive in 17 cases (23.9%), 33 cases (46.5%), and 21 cases (29.6%), respectively. The dominant overall intensity of LC3 expression (the most representative level of intensity in the cancer tissue as a whole) was negative, weakly positive, and strongly positive in nine cases (12.7%), 31 cases (43.65%), and 31 cases (43.65%), respectively (Table 1). Thus, the number of cases in which the individual cancer cells were weakly or strongly positive for LC3 was the same as the number of cases counted from the view of dominant overall intensity of LC3 expression.

We examined the difference in intensity level of LC3 expression in the peripheral area and central area of the pancreatic cancer tissue from all 71 cases (Table 2). We classified the pattern of intensity level into three groups according to whether the peripheral or central area contained more cells that stained immunohistochemically positive for LC3: (1) peripheral > central; (2) peripheral = central; and (3) peripheral < central. The peripheral intensity level of LC3 staining was stronger in 25 (40.3%) of the 62 cases that were positive for LC3 expression, and weaker in only two cases (3.2%), and LC3 expression in the peripheral area and central area was the same in 35 cases (56.5%). There was a trend toward a stronger level of intensity of LC3 expression in the peripheral area of the pancreatic cancer tissue, which included the invasive border.

To address the question of whether peripheral tumor cells with enhanced LC3 expression are under hypoxic stress, we carried out immunohistochemical staining using CA IX as a hypoxia marker on some representative cases. The results showed that in some cases the tumor cells with strong LC3 expression at the peripheral area concomitantly showed enhanced expression of CA IX (Fig. 4).

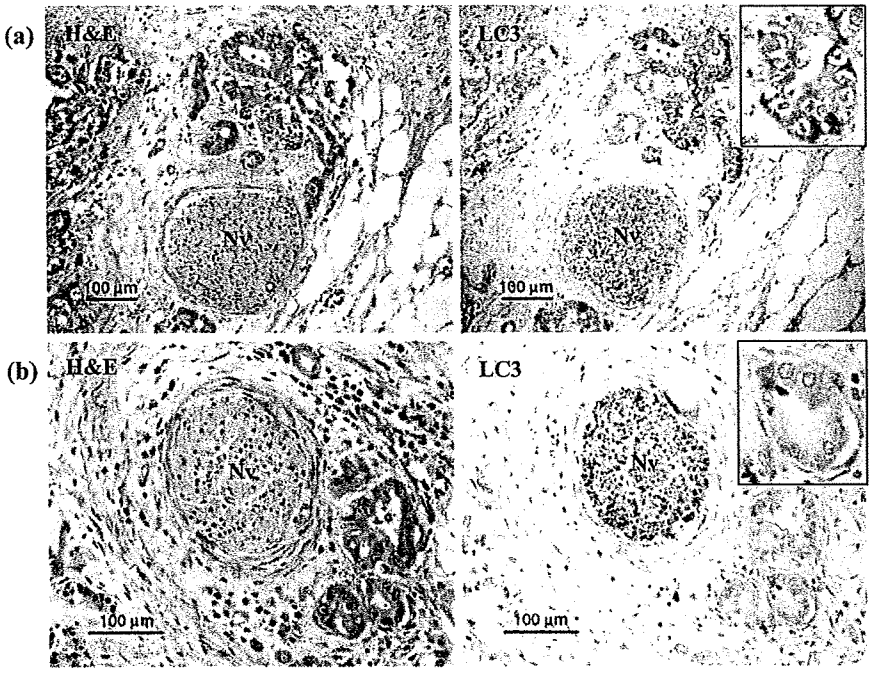

Fig. 2. LC3 protein was detected in pancreatic cancer tissue by immunohistochemical staining with LC3 antibody. Cancer tissue stained immunohistochemically with LC3 antibody and corresponding hematoxylin–eosin (HE)-stained sections are shown. A nerve cell (Nv) was used as an internal positive control to validate immunohistocheimical staining and evaluate the level of intensity of LC3 expression. The inserts are the photographs at higher magnification. (a) The cancer cells that stained as or more intensely for LC3 than the nerve cells were recorded as strongly positive. (b) The cancer cells that stained less intensely for LC3 than the nerve cells were recorded as weakly positive.

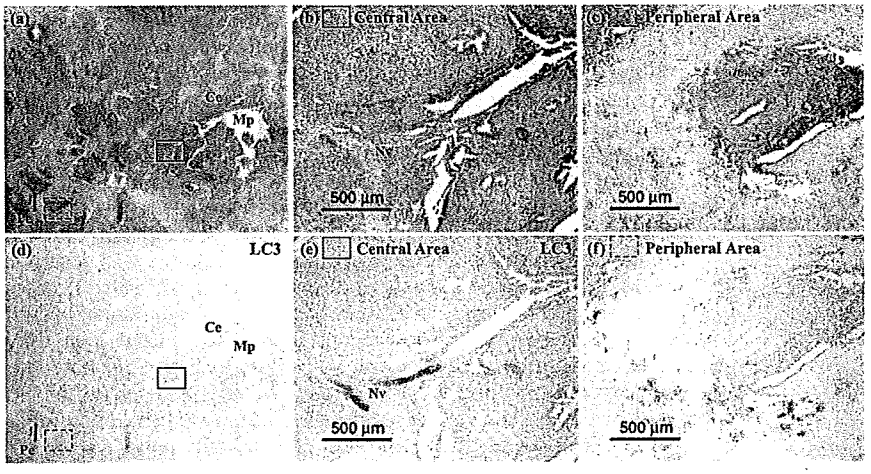

Fig. 3. A representative pancreatic tumor is shown. Cancer tissue (d–f) stained immunohistochemically with LC3 antibody and (a–c) corresponding hematoxylin–eosin (HE)-stained sections are shown. The peripheral area of the pancreatic cancer tissue (Pe) is more strongly positive for LC3 protein than the central area (Ce). Mp, main pancreatic duct; Nv, nerve cell.

Table 1. Intensity level of LC3 expression between the peripheral area and central area of the pancreatic cancer tissue, and the dominant overall intensity of LC3 expression of the pancreatic cancer tissue

Staining	Dominant intensity in the peripheral area (%)	Dominant intensity in the central area (%)	Dominant overall intensity (%)
Negative	9 (12.7)	17 (23.9)	9 (12.7)
Weakly positive	23 (32.4)	33 (46.5)	31 (43.65)
Strongly positve	39 (54.9)	21 (29.6)	31 (43.65)
Total cases	71 (100)	71 (100)	71 (100)

Table 2. Differences in the intensity level of LC3 expression in the peripheral area and central area of the pancreatic cancer tissue

No. cases	Pattern of intensity level		
	Peripheral > central (%)	Peripheral = central (%)	Peripheral < central (%)
62	25 (40.3)	35 (56.5)	2 (3.2)

Strong expression of LC3 in the peripheral area of the cancer tissue correlates with poor outcome and a short disease-free period. We analyzed the relationship between the intensity of LC3 expression (negative, weakly positive, strongly positive) in the peripheral area of pancreatic cancer tissue and overall survival. There was a trend toward the group with a strongly positive peripheral area to have a poor outcome ($P = 0.0579$) (Fig. 5a). We speculated that the cells strongly positive for LC3 in the peripheral area of the cancer tissue have a significant role in the characteristics of aggressive pancreas cancers and we divided the cases into two

doi: 10.1111/j.1349-7006.2008.00893.x

Fig. 4 Tumor cells with enhanced LC3 expression at the peripheral area concomitantly expressed carbonic anhydrase IX (CA IX) as a hypoxia marker. Three photographs of a representative case are shown (hematoxylin–eosin and CA IX and LC3 expression by immununohistochemical staining). The black arrows show the peripheral nerve at the peripheral area of the tumor tissue and which served as a positive internal control of LC3 expression.

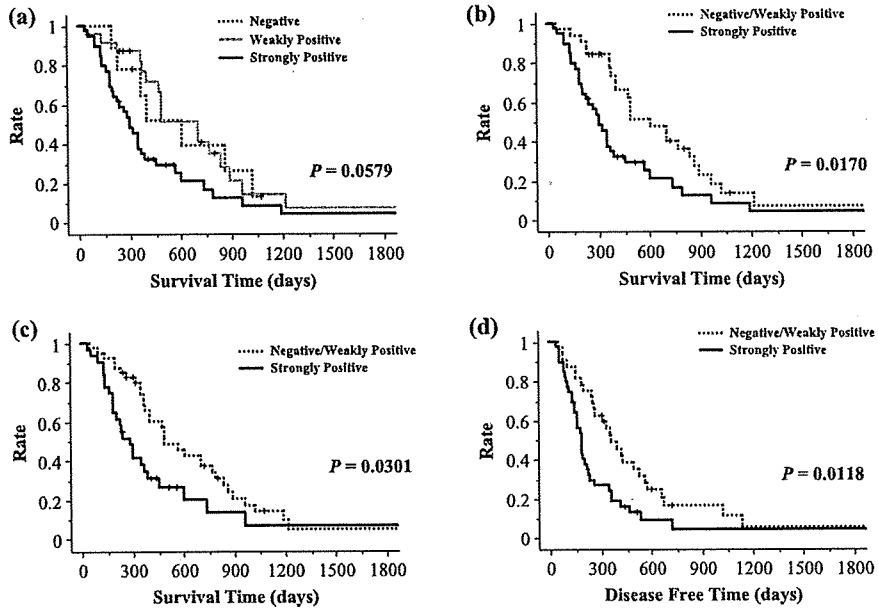

Fig. 5. Overall survival curves and disease-free curve according to the level of intensity of LC3 protein expression in the peripheral area and the dominant overall intensity of LC3 expression. (a) Overall survival curves according to the level of intensity of LC3 expression in the peripheral area of the cancer tissue in a negative group, weakly positive group, and strongly positive group. There was a trend for patients with strongly positive expression of LC3 protein to have a poor outcome ($P = 0.0579$). (b) Overall survival curves according to the level of intensity of LC3 protein expression in the peripheral area of the cancer tissue in the negative and weakly positive group and the strongly positive group. The group with strongly positive expression of LC3 protein had a significantly shorter survival time ($P = 0.0170$). (c) Overall survival curves according to the dominant overall intensity of LC3 protein expression in the negative and weakly positive group and the strongly positive group. The group with strongly positive expression of LC3 protein had a significantly shorter survival time ($P = 0.0301$). (d) Disease-free curves according to the level of intensity of LC3 protein expression in the peripheral area of the cancer tissue in the negative and weakly positive group and the strongly positive group. The group with strongly positive expression of LC3 protein in the peripheral area of the cancer tissue had a significantly shorter disease-free period ($P = 0.0118$).

groups, a negative or weakly positive group and a strongly positive group, according to the results for staining in the peripheral area. Interestingly, there was a significant correlation between the level of intensity of LC3 expression in the peripheral area of the cancer tissue and poor outcome ($P = 0.0170$) (Fig. 5b). Moreover, cases in which the dominant overall intensity of LC3 expression was strongly positive had a poorer outcome than the group in which the dominant overall intensity was weakly positive or negative ($P = 0.0301$) (Fig. 5c). Cases with a strongly positive intensity level in the peripheral area of the cancer tissue had a significantly shorter disease-free period than the cases with a negative or weakly positive intensity level ($P = 0.0118$) (Fig. 5d).

LC3 expression is correlated with clinicopathological factors, including tumor necrosis, differentiation, blood vessel infiltration, and tumor necrosis. In our study, there were significant correlations between a strong intensity of LC3 expression in the peripheral area, which included the invasive border, and a poor outcome and short disease-free survival time. In the next step, we investigated the relationship between LC3 expression and clinicopathological factors, including age, sex, tumor size, predominant differentiation, lowest differentiation, lymphatic vessel infiltration, blood vessel infiltration, intrapancreatic neural invasion, retroperitoneal invasion, UICC pT, UICC pN, UICC pStage, tumor necrosis, and nerve plexus invasion. The results showed significant correlations between the intensity level of LC3 expression in the peripheral area of the tumor and tumor size, predominant differentiation, lowest degree of differentiation, blood vessel infiltration, and tumor necrosis ($P < 0.05$) (Table 3), and two of the most significant correlations were with tumor size ($P = 0.0098$) or tumor necrosis ($P = 0.0127$) (Table 3).

Multivariate analyses of parameters significantly associated with overall survival. We carried out multivariate analyses to investigate the prognostic value of tumor size greater than 3.0 cm, predominantly poor differentiation, lowest degree of differentiation, 2 or 3 degrees of blood vessel infiltration, tumor necrosis and strongly positive intensity at the peripheral area, but only tumor size greater than 3.0 cm significantly increased the hazard ratio for overall survival

Table 3. Relationship between LC3 expression and clinicopathological factors of pancreatic cancer

	No. cases	LC3 expression			*P*-value
		N	W	S	
Age					
<65 years	37	3	10	24	
≥65 years	34	6	13	15	0.1875
Sex					
Male	40	5	13	22	
Female	31	4	10	17	0.9987
Tumor size					
<3.0 cm	34	3	17	14	
≥3.0 cm	37	6	6	25	0.0098
Predominant differentiation					
Well	25	5	13	7	
Moderately	37	3	8	26	0.0227
Poorly	9	1	2	6	
Lowest differentiation					
Well	8	2	5	1	
Moderately	27	2	11	14	0.0431
Poorly	36	5	7	24	
Lymphatic vessel infiltration					
0 or 1	50	6	19	25	
2 or 3	21	3	4	14	0.2940
Blood vessel infiltration					
0 or 1	7	1	5	1	
2 or 3	64	8	18	38	0.0497
Intrapancreatic neural invasion					
0 or 1	20	3	6	11	
2 or 3	51	6	17	28	0.1680
Retroperitoneal invasion					
0 or 1	27	4	12	11	
2 or 3	44	5	11	28	0.1567
UICC pT					
pT1 or pT2	4	1	1	2	
pT3	67	8	22	37	0.7415
UICC pN					
pN0	11	2	5	4	
pN1	60	7	18	35	0.4038
UICC pStage					
IA/IB/IIA	14	2	6	6	
IIB/III/IV	57	7	17	33	0.5805
Tumor necrosis					
Absent	50	7	21	22	
Present	21	2	2	17	0.0127
Nerve plexus invasion					
Absent	26	3	9	14	
Present	45	6	14	25	0.9450

N, negative; S, strongly positive; W, weakly positive.

($P = 0.0018$, hazard ratio = 2.8, 95% confidence interval = 1.4–5.2). None of the other factors significantly increased the hazard ratio for overall survival in the multivariate analyses.

Discussion

The clinicopathological significance of autophagy in cancer progression has remained unclear, and the role of autophagy in cell fate decisions remains a matter of controversy. Autophagy has been regarded as playing a role in providing nutrients by degrading existing cellular components. It is referred to as a recycling of cell constituents and an adaptive response to various cell stresses, such as energy deficiency.[10] Recently, the role of autophagy has also been shown to be an indispensable physiological reaction in caspase-independent programmed cell death (autophagic death), and autophagic cell death has been found to eliminate damaged and harmful cells, such as cancer cells damaged by anticancer reagents and cells infected with pathogenic microorganisms.[30,31] Paradoxically, autophagy has been proposed to be an indispensable physiological reaction for sustaining cell viability under nutrient-starved conditions.[10] In our previous study, we showed that colorectal cancer cells harbor functional autophagic machinery and that the autophagic machinery functions to prolong cell survival during shortages of nutrients.[25] The membrane-bound LC3-II protein level is used as a marker of autophagosome formation. We detected LC3-II by western blotting with the anti-LC3 antibody used in the previous study, and LC3 protein has also been detected in colon cancer cells by immunohistochemical staining.[25] We demonstrated that LC3 protein detected by immunohistochemical staining coincided with the localization of autophagosomes in colon cancer tissue specimens containing LC3 protein by electron microscopy and that autophagy contributes directly to cancer cell survival during nutrient starvation.[25] In a previous experiment, both an autolysosomal protease inhibitor and 3-methyladenine, an inhibitor of autophagosome formation, induced marked apoptotic death in all colorectal cancer cells examined.[25] However, the significance of excess expression of autophagic machinery in cancer tissue samples remained unclear. In the present study we showed that LC3 positivity of pancreatic cancer tissue was correlated with poor overall survival and a shorter disease-free period. Constitutive formation of autophagosomes in cancer cells may contribute to cell survival in the harsh cancer microenvironments in which cancers are known to progress.

On the other hand, autophagy may not be a causal step in malignant transformation at the cellular level and may instead be an indicator of a poor blood supply in the cancer microenvironment.[32] Interestingly, however, significant associations were found between the LC3 expression level in the peripheral area, which included the invasive margin, and several clinicopathological factors, including tumor size, predominant differentiation, lowest differentiation, blood vessel infiltration, and tumor necrosis. Multivariate analyses showed that the LC3 expression level in the peripheral area was not an independent prognostic factor, but that tumor size greater than 3.0 cm, which was the factor most significantly correlated with LC3 expression ($P = 0.0098$, Table 3), was significantly associated with poor overall survival. Moreover, there was a correlation between tumor necrosis and strong expression of LC3 in pancreatic cancer tissue ($P = 0.0127$; Table 3). Two cases showed decreased intensity of LC3 expression by immunohistochemical staining at the peripheral area (Table 2). Both of them showed an absence of tumor necrosis and the sizes of both tumors were less than 3 cm. Nine cases were totally negative for LC3 expression (Table 3). Only two cases (2.8%) were negative for LC3 expression and tumor necrosis, whereas 19 cases (26.8%) were positive for LC3 expression and tumor necrosis. Six cases (8.5%) were negative for LC3 expression and had a tumor size of 3.0 cm ≤ 0. Twenty-five cases (35.2%) were positive for LC3 expression and had a tumor size of ≤3.0 cm. Negative cases showed lesser tumor size (<3.0 cm) and an absence of tumor necrosis with significant correlations. These results suggest the functional significance of autophagy in pancreatic cancer tissue. This observation indicates that autophagy may promote cell viability in hypovascular pancreatic cancer tissue, where only limited oxygen and nutrient supplies would be expected. To address the question of whether peripheral tumor cells with enhanced LC3 expression are under hypoxic stress, we carried out immunohistochemical staining using CA IX as a hypoxia marker on some representative cases. There were some cases whose tumor cells with strong LC3 expression at the peripheral area showed concomitant enhanced expression of CA IX (Fig. 4). However, further studies are needed to address the relationship between autophagy and hypoxia, angiogenesis, and nutrient starvation by investigating a large

doi: 10.1111/j.1349-7006.2008.00893.x

number of cases and many kinds of cancer tissues. No LC3 expression was detected in the non-cancerous ductal epithelium of the pancreas in the present study (data not shown). We do not understand this discrepancy if autophagy is regarded as just a physiological response to poor blood supply. Moreover, as LC3 expression was significantly correlated with various clinicopathological factors, further study will be needed to determine its significance in relation to the malignant character of cancer cells.

Based on all of the above, taken together, we conclude that activated autophagy is associated with pancreatic cancer cells and that LC3 expression by pancreatic cancer cells is significantly correlated with a poor outcome. This is the first study to show the clinicopathological significance of autophagy in relation to a poor outcome and associations with clinicopathological parameters. It is speculated that autophagy may play a variety of pathophysiological roles in carcinogenesis, cancer progression, and metastasis, and that its role may vary with the cancer cell type due to differences in the characters of the cancer cells themselves and the microenvironment of the cancer tissue. To better understand the autophagic machinery for cancer cell survival related to carcinogenesis and cancer progression, we plan to extend our investigation to other cancer cell types by using cancer tissue samples.

Acknowledgments

This work was supported by a grant from the Ministry of Health, Labour, and Welfare for the Third-Term Comprehensive 10-year Strategy for Cancer Control. We wish to thank Miss Mai Okumoto for her excellent technical assistance.

References

1 Kumar V, Cotran RS, Robbins SL. *Robbins Pathologic Basis of Disease*, 5th edn. Philadelphia: W.B. Saunders, 1992.
2 Jain RK. Molecular regulation of vessel maturation. *Nat Med* 2003: **9**: 685–93.
3 Vaupel P, Thews O, Hoeckel M. Treatment resistance of solid tumors: role of hypoxia and anemia. *Med Oncol* 2001; **18**: 243–59.
4 Harris AL. Hypoxia – a key regulatory factor in tumour growth. *Nat Rev Cancer* 2002; **2**: 38–47.
5 Koong AC, Mehta VK, Le QT *et al.* Pancreatic tumors show high levels of hypoxia. *Int J Radiat Oncol Biol Phys* 2000; **48**: 919–22.
6 Buchler P, Reber HA, Lavey RS *et al.* Tumor hypoxia correlates with metastatic tumor growth of pancreatic cancer in an orthotopic murine model. *J Surg Res* 2004; **120**: 295–303.
7 Kitano M, Kudo M, Maekawa K *et al.* Dynamic imaging of pancreatic diseases by contrast enhanced coded phase inversion harmonic ultrasonography. *Gut* 2004; **53**: 854–9.
8 Izuishi K, Kato K, Ogura T, Kinoshita T, Esumi H. Remarkable tolerance of tumor cells to nutrient deprivation: possible new biochemical target for cancer therapy. *Cancer Res* 2000; **60**: 6201–7.
9 Esumi H, Izuishi K, Kato K *et al.* Hypoxia and nitric oxide treatment confer tolerance to glucose starvation in a 5′-AMP-activated protein kinase-dependent manner. *J Biol Chem* 2002; **277**: 32 791–8.
10 Levine B, Klionsky DJ. Development by self-digestion: molecular mechanisms and biological functions of autophagy. *Dev Cell* 2004; **6**: 463–77.
11 Tanida I, Minematsu-Ikeguchi N, Ueno T, Kominami E. Lysosomal turnover, but not a cellular level, of endogenous LC3 is a marker for autophagy. *Autophagy* 2005; **1**: 84–91.
12 Sener SF, Fremgen A, Menck HR, Winchester DP. Pancreatic cancer: a report of treatment and survival trends for 100 313 patients diagnosed from 1985 to 1995, using the National Cancer Database. *J Am Coll Surg* 1985; **189**: 1–7.
13 Geer RJ, Brennan MF. Prognostic indicators for survival after resection of pancreatic adenocarcinoma. *Am J Surg* 1993; **165**: 68–72.
14 Sohn TA, Yeo CJ, Cameron JL *et al.* Resected adenocarcinoma of the pancreas-616 patients: results, outcomes, and prognostic indicators. *J Gàstrointest Surg* 2000; **4**: 567–79.
15 Lim JE, Chien MW, Earle CC. Prognostic factors following curative resection for pancreatic adenocarcinoma: a population-based, linked database analysis of 396 patients. *Ann Surg* 2003; **237**: 74–85.
16 Kuhlmann KF, de Castro SM, Wesseling JG *et al.* Surgical treatment of pancreatic adenocarcinoma: actual survival and prognostic factors in 343 patients. *Eur J Cancer* 2004; **40**: 549–58.
17 Luttges J, Schemm S, Vogel I, Hedderich J, Kremer B, Kloppel G. The grade of pancreatic ductal carcinoma is an independent prognostic factor and is superior to the immunohistochemical assessment of proliferation. *J Pathol* 2000; **191**: 154–61.
18 Takai S, Satoi S, Toyokawa H *et al.* Clinicopathologic evaluation after resection for ductal adenocarcinoma of the pancreas: a retrospective, single-institution experience. *Pancreas* 2003; **26**: 243–9.
19 Takahashi S, Hasebe T, Oda T *et al.* Extra-tumor perineural invasion predicts postoperative development of peritoneal dissemination in pancreatic ductal adenocarcinoma. *Anticancer Res* 2001; **21**: 1407–12.
20 Mitsunaga S, Hasebe T, Iwasaki M, Kinoshita T, Ochiai A, Shimizu N. Important prognostic histological parameters for patients with invasive ductal carcinoma of the pancreas. *Cancer Sci* 2005; **96**: 858–65.
21 Kivelä AJ, Parkkila S, Saarnio J *et al.* Expression of transmembrane carbonic anhydrase isoenzymes IX and XII in normal human pancreas and pancreatic tumours. *Histochem Cell Biol* 2000; **114**: 197–204.
22 Shibaji T, Nagao M, Ikeda N *et al.* Prognostic significance of HIF-1 alpha overexpression in human pancreatic cancer. *Anticancer Res* 2003; **23**: 4721–7.
23 Sipos B, Weber D, Ungefroren H *et al.* Vascular endothelial growth factor mediated angiogenic potential of pancreatic ductal carcinomas enhanced by hypoxia: an *in vitro* and *in vivo* study. *Int J Cancer* 2002; **102**: 592–600.
24 Levine B. Cell biology: autophagy and cancer. *Nature* 2007; **446**: 745–7.
25 Sato K, Tsuchihara K, Fujii S *et al.* Autophagy is activated in colorectal cancer cells and contributes to the tolerance to nutrient deprivation. *Cancer Res* 2007; **67**: 9677–84.
26 Sobin HL, Wiitekind C, eds. *TNM Classification of Malignant Tumors*, 6th edn. New York: Wiley-Liss, 2002.
27 Hamilton RS, Aaltonen AL, eds. *World Health Organization Classification of Tumours. Pathology and Genetics of Tumors of the Digestive System.* Lyon: IARC Press, 2000.
28 Japan Pancreas Society. *The Classification of Pancreatic Carcinoma*, 1st English edn. Tokyo: Kanehara, 1996.
29 Jäger S, Bucci C, Tanida I *et al.* Role for Rab7 in maturation of late autophagic vacuoles. *J Cell Sci* 2004; **117**: 4837–48.
30 Kirkegaard K, Taylor MP, Jackson WT. Cellular autophagy: surrender, avoidance and subversion by microorganisms. *Nat Rev Microbiol* 2004; **2**: 301–14.
31 Kondo Y, Kanzawa T, Sawaya R, Kondo S. The role of autophagy in cancer development and response to therapy. *Nat Rev Cancer* 2005; **5**: 726–34.
32 Klionsky DJ, Abeliovich H, Agostinis P *et al.* Guidelines for the use and interpretation of assays for monitoring autophagy in higher eukaryocytes. *Autophagy* 2008; **4**: 151–75.

[Autophagy 4:5, 692-700; 1 July 2008]; ©2008 Landes Bioscience

Research Paper

Loss of Pten, a tumor suppressor, causes the strong inhibition of autophagy without affecting LC3 lipidation

Takashi Ueno,[1] Wataru Sato,[2] Yasuo Horie,[2] Masaaki Komatsu,[1] Isei Tanida,[1,†] Mitsutaka Yoshida,[3] Shigetoshi Ohshima, Tak Wah Mak,[4] Sumio Watanabe[2,‡] and Eiki Kominami[1,*]

[1]The Department of Biochemistry and [3]Division of Ultrastructural Research; Juntendo University School of Medicine; Hongo, Tokyo Japan; [2]The Department of Gastroenterolog Akita University; Akita, Japan; [4]The Campbell Family Institute for Breast Cancer Research; Toronto, Ontario Canada

[†]Present address: Department of Biochemistry and Cell Biology; National Institute of Infectious Disease; Tokyo, Japan

[‡]Present address: Department of Gastroenterology; Juntendo University School of Medicine; Tokyo, Japan

Abbreviations: Pten, phosphatase and tensin homologue deleted on chromosome ten; PI3-kinase, phosphatidylinositol 3-kinase; PtdIn phosphatidylinositol; PtdIns(4,5)P_2, phosphatidylinositol (4,5)-bisphosphate; PtdIns(3,4)P_2,phosphatidylinositol (3,4)-bisphosphat PtdIns(3,4,5)P_3, phosphatidylinositol (3,4,5)-trisphosphate; Akt, protein kinase B; RT, real time; PCR, polymerase chain reaction; FCS, fet calf serum; Williams E/10% FCS, Williams' medium E containing 10% FCS; PBS, 20 mM Na-phosphate, pH 7.4, 0.15 M NaCl; E64 ethyl-(+)-(2S,3S)-3-[(S)-methyl-1-(3methyl-butyl-carbamoyl)-butylcarbamoyl]-2-oxiranecarboxylate; MAP, microtubule associated protei LC3, light chain 3; LC3-I, solubleform of light chain 3; LC3-II, lipidated form of light chain 3; GABARAP, γ-aminobutyric acid$_A$ recepto assoiciated protein; GST, glutathione S-transferase; MBP, maltose binding protein; BHMT, betaine homocysteine methyltransferase; SD sodium dodecylsulfate; PAGE, polyacrylamide gel electrophoresis; mTor, mammalian target of rapamycin; LGP85, lysosomal membra glycoprotein 85

Key words: autophagy, Pten, autophagosome, autolysosome, class I phosphatidylinositol-3-kinase, Akt

[1]**Pten (phosphatase and tensin homolog deleted on chromosome ten), a tumor suppressor, is a phosphatase with a variety of substrate specificities. Its function as a negative regulator of the class I phosphatidyl-inositol 3-kinase/Akt pathway antagonizes insulin-dependent cell signaling. The targeted deletion of Pten in mouse liver leads to insulin hypersensitivity and the upregulation of the phosphatidyl-inositol 3-kinase/Akt signaling pathway. In this study, we investigated the effects of Pten deficiency on autophagy, a major cellular degradative system responsible for the turnover of cell constituents. The autophagic degradation of [^{14}C]-leucine-labeled proteins of hepatocytes isolated from Pten-deficient livers was strongly inhibited, compared with that of control hepatocytes. However, no significant difference was found in the levels of the Atg12-Atg5 conjugate and LC3-II, the lipidated form of LC3, an intrinsic autophagosomal membrane marker, between control and Pten-deficient livers. Electron microsopic analyses showed that numerous autophagic vacuoles (autophagosomes plus autolysosomes) were present in the livers of control mice that had been starved for 48 hours, whereas they were markedly reduced in Pten-deficient livers under the same conditions. In vivo administration of leupeptin to control livers caused the inhibition of autophag proteolysis, resulting in the accumulation of autolysosomes. The autolysosomes could be separated as a denser autolysosom fraction from other cell membranes by Percoll density gradie centrifugation. In leupeptin-administered mutant livers, howeve the accumulation of denser autolysosomes was reduced substa tially. Collectively, we conclude that enhanced insulin signaling i Pten deficiency suppresses autophagy at the formation and matur tion steps of autophagosomes, without inhibiting *ATG* conjugatio reactions.**

Introduction

Insulin plays a critical role in controlling glucose and lipid metal olism in liver, muscle and adipose tissues. In muscle and adipo tissue, insulin promotes glucose uptake from circulating blood cells, resulting in a decrease in blood glucose levels. In liver, insul stimulates glycogen synthesis, glycolysis, fatty acid synthesis a protein synthesis. The binding of insulin to insulin receptors induc a series of complex cell signaling pathways, in which the class I pho phatidylinositol 3-kinase (PI3-kinase)/Akt plays a key role, upstrea in the pathway. The insulin signal causes the activation of class PI3-kinase.[1-3] Activated class I PI3-kinase phosphorylates phosphat dylinositol 4-phosphate and phosphatidylinositol (4,5)-bisphospha (PtdIns(4,5)P_2) to form phosphatidylinositol (3,4)-bisphospha (PtdIns(3,4)P_2) and phosphatidylinositol (3,4,5)-trisphospha (PtdIns(3,4,5)P_3), respectively.[4] Both PtdIns(3,4)P_2 andPtdIns(3,4, P_3 bind to Akt (protein kinase B) and its activator phosphoinositid dependent kinase-1.[5,6] Activated Akt is required for the subseque

*Correspondence to: Eiki Kominami; Department of Biochemistry; Juntendo University School of Medicine; Building 9; Rm. 913; 2-1-1 Hongo; Bunkyo-ku, Tokyo 113-8421 Japan; Tel.: +81.3.5802.1030; Fax: +81.3.5802.5889; Email: komilabo@med.juntendo.ac.jp

Submitted: 01/18/08; Revised: 04/09/08; Accepted: 04/10/08

Previously published online as an *Autophagy* E-publication: http://www.landesbioscience.com/journals/autophagy/article/6085

inactivation of glycogen synthase kinase 3β, which eventually leads to the stimulation of glycogen synthesis and fatty acid synthesis.[7] Activated Akt also stimulates the mTor /P70S6-kinase pathway, the activation of which is required for the initiation of protein synthesis.[8,9] Pten is a tumor suppressor, with multifunctional phosphatase activity.[10] Pten specifically dephosphorylates PtdIns(3,4,5)P_3 to produce PtdIns(4,5)P_2, thus functioning as a negative regulator of the class I PI3-kinase/Akt pathway.[11] It has been reported that Pten is frequently mutated in many cancer cells. The inactivation of Pten results in hyper activation of the class I PI3-kinase/Akt pathway, which is closely correlated with the dysregulation of cell proliferation.

Autophagy is a catabolic system that plays a major role in the turnover of cell constituents, including organelles and cytosolic proteins.[12,13] Autophagy has been most fully investigated in the liver. Under nutrient-rich conditions, autophagy proceeds at the basal rate (~1.5% of total liver protein/hour). Under starvation conditions, the rate is enhanced ~3-fold to a maximal level (~4–5% of the total liver protein/hour).[14] In nutrient starved cells, numerous autophagosomes engulfing cytoplasmic organelles (mitochondria, endoplasmic reticulum, ribosomes, etc.,) and soluble cytosolic proteins are formed. The autophagosome then fuses with a lysosome to mature into an autolysosome, in which sequestered cytoplasmic components are degraded by lysosomal hydrolases. More than 20 *ATG* genes that are essential for autophagy have been identified and characterized to date.[15,16] Many of the *ATG* genes play pivotal roles in two ubiquitylation-like protein conjugation systems.

Autophagy is distinctly controlled by two different classes of PI3-kinase.[17] The stimulation of class I PI3-kinase activity inhibits autophagy, whereas the class III PI3-kinase that phosphorylates PtdIns to produce PtdIns(3)-phosphate is required for autophagy. It has been reported that feeding HT-29 cells with synthetic lipids dipalmitoyl PtdIns(3,4)P_2 and dipalmitoyl PtdIns(3,4,5)P_3 or the activation of class I PI3-kinase by interleukine 13 causes a significant inhibition in autophagy, whereas feeding synthetic dipalmitoyl PtdIns(3)-phosphate, a class III PI3-kinase product, stimulates autophagy.[18] In fact, the overexpression of wild-type Pten in HT-29 cells reversed the inhibitory effect of autophagy by interleukine 13, whereas the overexpression of a mutant form of Pten, which lacks phosphoinositide phosphatase activity, failed to reverse the inhibition of autophagy.[19] In addition, overexpression of the constitutively active form of Akt in HT-29 cells caused the inhibition of autophagy, whereas the overexpression of the constitutively inactive form of Akt caused the activation of autophagy.[19] These results suggest that the signaling pathway downstream from Akt is important for the negative control of autophagy. In the yeast *Saccharomyces cerevisiae*, PI3-kinase Vps34 forms two distinct protein complexes. One complex, comprised of Vps34/Vps15/Atg6(Vps30)/Vps38, functions in post-Golgi membrane transport and the other complex, comprised of Vps34/Vps15/Atg6(Vps30)/Atg14, functions in autophagy.[20] In mammals, class III PI3-kinase, a mammalian homologue of yeast Vps34, forms a complex with beclin 1(mammalian Atg6 homologue) in the trans Golgi network[21] and this complex formation has been shown to be essential for autophagy.[21,22] In contrast to the essential role of the class III PI3-kinase in autophagy, the molecular mechanism, by which autophagy is inhibited by the class I PI3-kinase, is not fully understood. In particular, little is known as to which of the three steps of autophagy, i.e., autophagosome formation, the maturation of autophagosomes into autolysosomes, and autolysosomal degradation, is most affected by the stimulation of the class I PI3-kinase/Akt pathway. In order to address this issue, we identified an animal model in which the class I PI3-kinase is constitutively activated thus permitting autophagy to be suppressed, irrespective of the nutrient conditions.

Hepatocyte-specific Pten-deficient mice were a useful experimental system for investigating the effects of hyper activation of the class I PI3-kinase/Akt pathway on metabolism.[23,24] As expected, the loss of Pten function elicited insulin hypersensitivity with elevated levels of phosphorylated Akt and led to tumorigenesis, the development of adenomas and hepatocellular carcinomas.[24] Unexpectedly the Pten deficiency induced diverse genes that are involved in fatty acid synthesis and β-oxidation, resulting in a fatty liver and steatohepatitis with accumulated triglycerides.[23,24] Using this animal model, we investigated the effects of a Pten deficiency on hepatocyte autophagy, focusing our attention on each step of autophagy, i.e., the formation of autophagosomes, the maturation of autophagosomes into autolysosomes, and autolysosomal degradation.

Results

Degradation of long-lived proteins under starvation conditions To assess quantitative effects of Pten deficiency on autophagy, we first examined the degradation of long-lived proteins of cultured hepatocytes. Figure 1A summarizes the data for the degradation of long-lived hepatocyte proteins labeled with ^{14}C-leucine for 22 h. In control hepatocytes, the degradation was markedly enhanced under starvation conditions (upper left-side box, lane A vs. upper right-side box, lane A). Under starvation conditions, the degradation was effectively inhibited in the presence of 3-methyladenine, a specific inhibitor of autophagy (lane B), E64d plus pepstatin, lysosomal proteinase inhibitors (lane C), 5 mM methylamine (lane D) and 20 mM NH_4Cl (lane F) that neutralize lysosomal lumenal pH. The simultaneous addition of E64d plus pepstatin and methylamine or NH_4Cl to the chase medium maximally inhibited protein degradation (lanes E and G). In contrast, the degradation in Pten-deficient hepatocytes was substantially inhibited. No large difference was found between starved and non-starved conditions and, the fraction of degradation sensitive to lysosomal proteinase inhibitors in Pten-deficient hepatocytes (~3–4% under starvation conditions, lower left-side box) was much smaller than that in control hepatocytes (~7–8% under starvation conditions, upper left-side box). These data clearly demonstrate that autophagic protein degradation is markedly diminished in Pten-deficient hepatocytes.

The magnitude of the inhibition of autophagic protein degradation in Pten-deficient hepatocytes was comparable to that of autophagy-deficient hepatocytes, in which Atg7, an E1-like enzyme, which is essential for autophagy, was deleted.[34] It is generally thought that the activation of Akt stimulates the mTor /P70S6-kinase pathway the activation of which causes the suppression of autophagy.[17] We therefore reasoned that the inhibition of autophagy could be mediated through activation of the mTor/P70S6-kinase pathway by a Pten-deficiency. We surveyed the phosphorylation state of Akt the ribosomal S6 subunit, and initiation factor 4E-binding protein by immunoblotting (Fig. 1B). As expected, all of these molecules

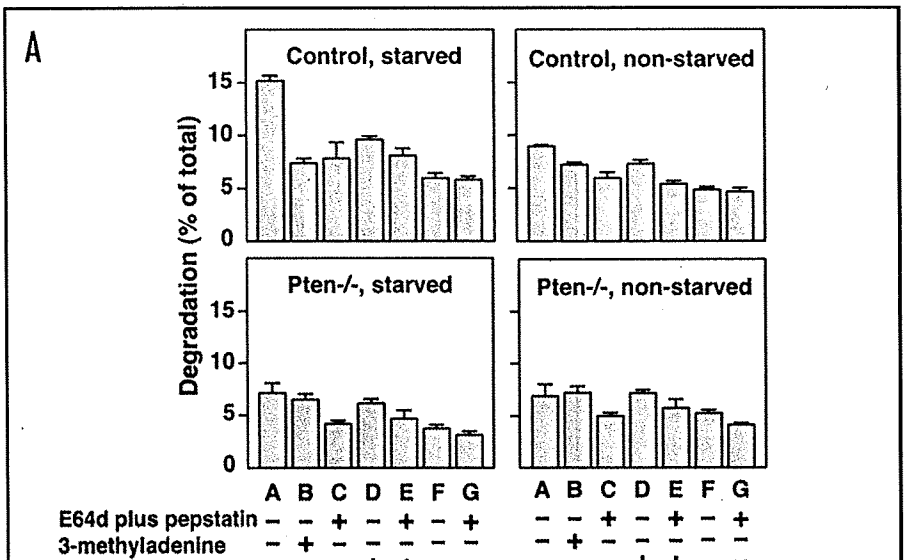

Figure 1. Degradation of long-lived proteins of control and Pten-deficient hepatocytes under starved and non-starved conditions. (A) Hepatocytes isolated from control and Pten-deficient livers were cultured in Williams E/10% FCS. The cells were then incubated with Williams E/10% FCS containing [^{14}C]-leucine (0.5 μCi/ml) for 22 h to label the long-lived proteins. The cells were then washed with Williams E/10% FCS containing 2 mM unlabelled leucine and incubated with the medium for 2 hours. The cells were washed with PBS and incubated for 4 hours with either Krebs-Ringer bicarbonate buffer (left-side boxes, starved) or Williams E/10% FCS (right-side boxes, non-starved) in the presence (lanes B to G) or absence (lane A) of various inhibitors. The inhibitors added were: 10 mM 3-methyladenine (lane B), 10 μg/ml E64d and 10 μg/ml pepstatin (lane C), 5 mM methylamine (lane D), 5 mM methylamine plus 10 μg/ml E64d and 10 μg/ml pepstatin (lane E), 20 mM NH_4Cl (lane F) and 20 mM NH_4Cl plus 10 μg/ml E64d and 10 μg/ml pepstatin (lane G). At the end of the incubation, trichloroacetic acid-soluble radioactivity released in the medium and trichloroacetic acid-insoluble radioactivity remaining in the cells were determined separately as described in Materials and Methods. Degradation (% of total) determined in triplicate assay, is expressed as the mean (%) ± S.D. (B) Whole liver lysates from control (+/+) and Pten-deficient (-/-) mice starved for 12 h were separated in SDS-polyacrylamide gels and the separated proteins were electrophoretically transferred to a PVDF membrane. Pten, Akt, phosphorylated Akt, phosphorylated ribosomal S6 and initiation factor 4E-binding protein were determined by immunoblotting analysis using respective antibodies. (C) Long-lived proteins of control and Pten-deficeint hepatocytes were labeled with [^{14}C]-leucine (0.5 μCi/ml), chased with Williams E/10% FCS containing 2 mM unlabelled leucine for 2 h, and incubated with either Krebs-Ringer bicarbonate buffer (KRB) or Williams E/10% FCS in the presence of absence of 0.2 mM rapamycin for 4 hours. Degradation (% of total) determined in triplicate is expressed as the mean (%) ± S.D.

were in the phosphorylated state in starved Pten deficient livers, while they were dephosphorylate in control livers (Fig. 1B).

We next tested whether or not rapamyci could enhance autophagic protein degradatio in Pten-deficient hepatocytes under nutrient-ric conditions. Rapamycin is known to inactivat mTor and induce autophagy even under nutrient rich conditions. When rapamycin was adde to the chase medium under both starved an non-starved conditions, rapamycin substan tially enhanced protein degradation in contr hepatocytes under non-starved conditions to level almost equivalent to that obtained unde starved conditions. In contrast, no significar enhancement was observed with Pten-deficier hepatocytes under both starved and non-starve conditions (Fig. 1C). Thus, inactivation of mTo P70S6-kinase pathway by rapamycin was n sufficient for reversing autophagy suppression i Pten-deficient livers.

Expression of *ATG* genes in wild type an Pten-deficient livers. We next examined the poss bility that hyper-activation of Akt in Pten-deficie livers may suppress the expression of *ATG*. comprehensive DNA microarray using mRN isolated from control and Pten-deficient mou hepatocytes revealed that expression of som *ATG* genes was substantially decreased in muta hepatocytes, compared with control hepatocyt (data not shown). This was further confirme by RT-PCR analysis (Fig. 2A). *ATG7*, *ATG3* an *ATG10* are genes that encode E1-like enzym (Atg7) and E2-like enzymes (Atg3 and Atg10 respectively, which participate in the autophag specific protein conjugation system.[15,16] The expression was decreased by 20–60% in Pte deficient hepatocytes, compared with contr hepatocytes. The expression of two gene *ATG12* and *MAP-LC3*, which encode modifie (Atg12 and LC3) of the two *ATG* conjugatio systems, was also decreased to less than 50% i mutant hepatocytes, whereas expression of *ATG (BECLIN)* and *ATG16* was less affected. Thus, Pten-deficiency or hyper-activation of the class PI3-kinase/Akt pathway elicited the downregul tion of transcription of some *ATG* genes that a essential to autophagy.

The decrease in the transcription level of the *ATG* genes, however, did not parallel the chang in protein levels of the *ATG* gene product Figure 2B shows immunoblotting analyses da for liver homogenates. A Pten-deficiency cause hepatomegaly[23,24] and the total liver protein mutant livers was increased by 30–50%, compare with that of control livers. Therefore, the amoun of protein loaded onto SDS-polyacrylamide ge

were arranged so that the levels of *ATG* gene products per liver could be directly compared. Contrary to the data on message levels (Fig. 2A), significantly more Atg7, Atg3, Atg10 and Atg12-Atg5 conjugate were present in Pten deficient livers than in control livers (Fig. 2B). This was also the case for LC3 expression between control and mutant livers. Intriguingly, both LC3-I and LC3-II were present in Pten-deficient livers and in the control livers. LC3-I is a soluble form with a free carboxyl terminal glycine, while LC3-II is a lipidated form with its carboxyl-terminal glycine conjugated with phosphatidylethanolamine. Since it is the latter form of LC3 that is recruited onto autophagosomal membranes, the results indicate that autophagy-specific protein conjugation reactions function normally in Pten-deficient livers. In order to examine intracellular distribution of LC3-I and LC3-II, liver homogenate was separated in mitochondrial/lysosomal, microsomal and cytosolic fractions (Fig. 2C). There was no significant difference in the distribution of LC3-I and LC3-II between control and Pten-deficient livers. LC3-II was most abundant in mitochondrial/lysosomal fraction, whereas LC3-I was mainly present in the cytosolic fraction (Fig. 2C).

Morphological analysis of autophagic vacuoles in wild type and Pten-deficient livers. As LC3-II was expressed normally in mutant livers, it is important to determine whether or not autophagosomes can be formed in mutant livers under starvation conditions. The administration of leupeptin, a potent inhibitor of lysosomal cysteine proteinases, to rats and mice is known to cause the accumulation of autophagic vacuoles (autophagosomes and autolysosomes) by inhibiting lysosomal proteolysis.[35-37] We therefore injected leupeptin, as described in the Materials and Methods section, into both control and mutant mice that had been starved for 48 hours. One hour after the injection, the livers were subjected to perfusion-fixation with glutaraldehyde and examined by electron microsopy. Figure 3 shows that autophagic vacuoles were abundantly present in control livers (A and C), but only a few were observed in mutant livers (B and C). Morphometry revealed that the number of autophagic vacuoles per 100 μm^2 of hepatocyte cytoplasm in control livers is 44.37 + 13.66 (mean + S.D., n = 30) whereas that in mutant livers is 11.78 + 8.6 (mean + S.D., n = 30) (Fig. 3E). Interestingly, some vacuoles in mutant livers possessed lumenal structures with sequestered components shrunken to the center of the vacuoles (Fig. 3D, arrows). In contrast, the sequestered components in most of the vacuoles in control livers appeared to have blurred lumenal structures, suggesting that the vacuoles consist of typical autolysosomes. Thus, the accumulation of autophagic vacuoles is severely hindered in Pten-deficient livers, compared with control livers, consistent with biochemical data showing that the starvation-enhanced degradation of long-lived protein is markedly suppressed by the loss of Pten.

Assessment of autolysosomes in control and mutant livers. The decreased number of autophagic vacuoles may reflect a reduction in autophagosome formation and/or the retardation of autophagosome maturation to autolysosome. Because the levels of LC3-II, an autophgaosomal membrane marker, were slightly increased, but total number of autophagic vacuoles was markedly decreased in Pten-deficient livers, compared to control livers, we hypothesized that the autophagy dysfunction in the Pten-deficiency could be primarily attributed to an impairment in autophagosome formation. Additionally, another possibility for an impairment of autophagosome maturation into autolysosome should also be considered. In

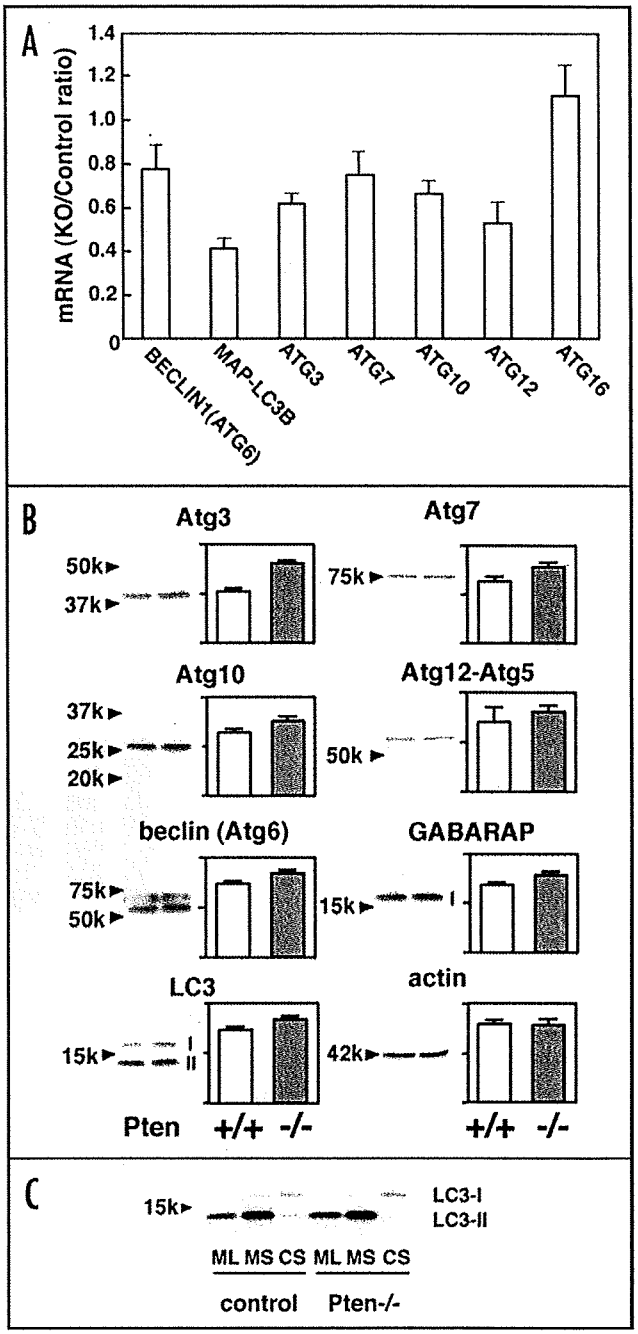

Figure 2. Expression of *ATG* gene products in control and Pten-deficien livers. (A) Messenger RNAs extracted from control and Pten-deficient liver were subjected to RT-PCR analysis as described in Materials and Methods The expression levels of mRNAs were determined for some representative *ATG* genes and the ratios of the levels between Pten-deficient livers (KO and control livers (Control) were plotted. (B) Immunoblotting was performed with whole cell lysates from control and Pten-deficient livers. As the total liver protein of mutant livers was 1.3-fold higher than that of control livers due to hepatomegaly, 26 µg protein of mutant liver lysate and 20 µg protein o control lysate were run in 10% or 12.5% SDS-polyacrylamide gels and the separated polypeptides were subjected to immunoblotting analyses. Data shown are representative of three separate experiments. Quantitative densitometry was performed using NIH imaging system. As for LC3, the data for LC3-II are shown. (C) Mitochondrial/lysosomal (ML), microsomal (MS), and cytosol (S) fractions were isolated from normal and Pten-deficient livers as described in Materials and Methods. Twenty five microgram protein of each fraction was separated on 12.5% SDS-polyacrylamide gels and subjected to immunoblotting analysis using anti-LC3 antibody.

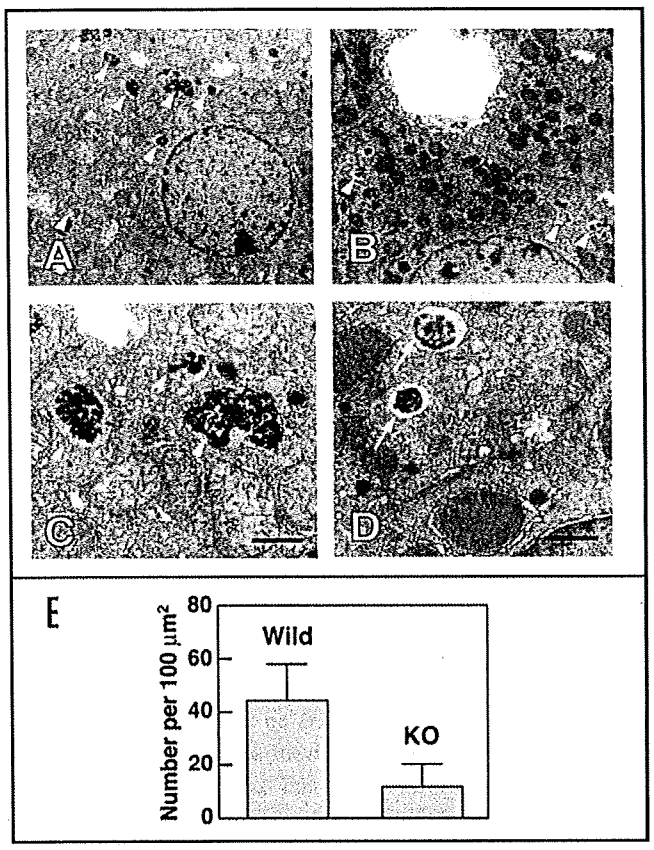

Figure 3. Electron microscopic examination of control and Pten-deficient livers. Normal control and liver-specific Pten-deficeint mice were starved for 48 hours and leupeptin (0.15 mg/10 g body weight) was injected intraperitoneally. One hour later, the livers were perfusion-fixed and subjected to electron microscopic analyses as described in Materials and Methods. Autophagic vacuoles accumulating in the cytoplasm of control hepatocytes (A and C) and mutant hepatocytes (B and D) are shown by arrowheads. Bar, 1 μm. E. Morphometric analysis of autophagic vacuoles was performed with 30 different areas of the cytoplasm of control and mutant hepatocytes. Numbers of the vacuoles per 100 μm² cytoplasm were expressed as the mean ± S.D.

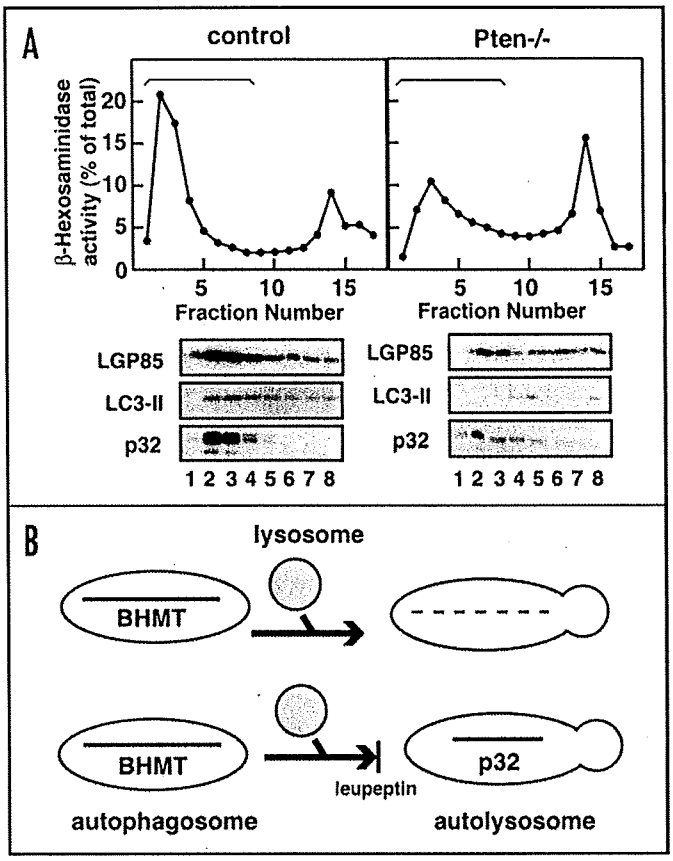

Figure 4. Density-shift of leupeptin-inhibited autolysosomes revealed b Percoll gradient centrifugation. (A) Liver mitochondrial/lysosomal fractic (35 mg protein) isolated from control (+/+) and Pten-deficient (-/-) mic starved for 48 hours was loaded onto 53% Percoll in 5 mM Tes-NaOH (p 7.5)-0.3 M sucrose and centrifuged at 50,000 x g for 40 min. After centrif gation, 1.5 ml fractions were collected from the bottom (No. 1) to the tc (No. 17). Beta-hexosaminidase activity was assayed and plotted in upp line graphs. Total activity recovered was 565 μmole/min (control) and 49 μmole/min (Pten-deficient), respectively. Distribution of LGP85, LC3-II, ar the p32 fragment of BHMT (p32) in the denser autolysosome fractions (N 1–No. 8) were determined by immunoblotting analysis. (B) Schematic pr sentation showing how a p32 fragment of BHMT accumulates in leupepti treated autolysosomes. In the absence of leupeptin, the BHMT sequestere in autophagosomes is completely degraded upon fusion of autophagosom with the lysosomes to form autolysosomes (upper route). In the presence leupeptin, BHMT is degraded to form a 32 k-Da fragment, which remains the autolysosomal lumen (lower route). For details, see reference 27.

order to examine this possibility further, we conducted a density-shift assay of autolysosomes on Percoll gradients.

When leupeptin was intraperitoneally administered to starved rats or mice, it was preferentially incorporated into hepatocyte lysosomes, eliciting considerable inhibition of autolysosomal proteolysis.[35-41] As a consequence, autolysosomal turnover was also inhibited, resulting in the accumulation of autolysosomes holding sequestered components in their lumen.[38-41] Due to the accumulated autophagic substrates in the lumen, the density of these autolysosomes was higher than other cell organelles and membranes, thus enabling them to be separated by Percoll gradient centrifugation.[39-41] We isolated mitochondrial/lysosomal fractions from leupeptin-administered control and mutant livers. The mitochondrial/lysosomal fraction, as isolated, was loaded onto isotonic 53% Percoll and centrifuged as described in the Materials and Methods section. As the distribution of lysosomal β-hexosaminidase activity as well as LGP85 and LC3-II shows, the denser autolysosomes were separated in fractions No. 1 to No.8 (Fig. 4A, left) in the control livers. More than 60% of the β-hexosaminidase activity was recovered in the lower autolysosomal fractions. In contrast, the accumulation of denser autolysosomes was significantly inhibited and ~40% of the β-hexosaminidase activi was recovered in autolysosomal fractions in the Pten-deficient liver (Fig. 4A, right) We previously found that betaine homocystein methyltransferase was sequestered in the autophagosomal lume together with other cytoplasmic proteins in the liver.[27] The enzym was immediately degraded by lysosomal proteinases upon maturatic of autophagosomes into autolysosomes. In the presence of leupepti however, the degradation ceased to accumulate a 32 k-Da fragmer (p32) of the enzyme as a partially digested intermediate (Fig. 4B As the production of p32 is dependent on the inhibition of cyctein proteinases by leupeptin, p32 can be used as a convenient marker f autolysosomes accumulating in the presence of leupeptin. As show in Figure 4A, distribution of p32 coincides with those of LGP8 and LC3 in these fractions obtained from control livers. In contras

weaker signals of LC3-II and LGP85 as well as p32 were detected in these fractions of mutant specimens. These data indicate that autophagosome maturation into autolysosomes is also substantially inhibited in Pten deficient livers.

Discussion

Hepatocyte-specific Pten-deficient mice have lower glucose levels than wild type mice and exhibit hyper insulin sensitivity,[23,24] indicating that a hepatic Pten deficiency exerts profound effects on the entire metabolism of the body. As expected, phosphorylated Akt and MAPK, two signaling molecules that are located downstream of class I PI3-kinase, were markedly increased in Pten-deficient hepatocytes, compared to control hepatocytes.[23,24] Thus, the loss of Pten function in the liver caused the constitutive activation of the class I PI3-kinase/Akt pathway.

The findings herein show that the autophagic protein degradation of long-lived proteins is strongly suppressed in Pten-deficient hepatocytes, compared to control hepatocytes. The magnitude of the suppression was almost equivalent to that of Atg7-deficient hepatocytes.[34] Our data are consistent with the previous observations of colon cancer HT29 cells, in which the class I PI3-kinase/Akt pathway was activated by incubating the cells with dipalmitoyl PtdIns(3,4,5)P_3, a class I PI3-kinase product, but not with dipalmitoyl PtdIns(4,5)P_2, leading to the inhibition of autophagic protein degradation.[18] Activation of Akt stimulates the mTor/P70S6-kinase pathway and the activation of mTor/P70S6-kinase pathway induces suppression of autophagy.[17] We confirmed that both ribosomal S6 and initiation factor 4E-binding protein, downstream components of the mTor/P70S6-kinase pathway, were phosphorylated in starved Pten-deficient livers. However, rapamycin, which induces autophagic protein degradation of control hepatocytes even under non-starved conditions by inhibiting mTor/P70S6-kinase pathway, did not stimulate protein degradation of Pten-deficient hepatocytes. Thus, autophagy suppression of Pten-deficient hepatocytes cannot be explained as a result of chronic activation of the mTor/P70S6-kinase pathway, but rather may be attributable to some mTor-independent mechanism that has yet to be understood. Transcription regulation by Foxo3 has been proposed recently as a potential mechanism for controlling the ubiquitin-proteasome system and autophagy in skeletal muscles.[42,43] Activated Akt phosphorylates Foxo3 and inhibits its transcriptional functions by keeping Foxo3 away from the nucleus. Dephosphorylated Foxo3 stimulates the transcription of autophagy-related genes—including some ATG genes. It has been also found that a trimeric GTP-binding protein G_{i3} mediates insulin-dependent suppression of autophagy in the rat liver.[44] Connection between activated class I PI3-kinase and G_{i3} may be also considered. Further investigations are necessary to clarify the mechanism by which hyperactivation of the class I PI3-kinase in Pten-deficient mouse livers causes suppression of autophagy.

RT-PCR analysis indicated that the transcription of some *ATG* genes that are involved in the *ATG* conjugation system was significantly decreased. We therefore speculated that chronic activation of Akt might cause the direct inhibition of the *ATG* conjugation reaction. However, the decreased expression of such messages was not connected to a decrease in translation: the cellular levels of these gene products were increased slightly in Pten-deficient livers compared to a normal control. Notably, the levels of Atg12-Atg5 conjugate are higher in mutant livers than in control livers, and LC3 is present in both the free (LC3-I) and lipidated form (LC3-II) in both livers. Furthermore, cell fractionation analysis revealed that there is no significant difference in intracellular distribution of LC3-I and LC3-II between normal and Pten-deficient livers (Fig. 2C). These data clearly indicate that the loss of Pten does not affect *ATG* conjugation reactions per se. The slight increase in the levels of these Atg proteins may reflect a compensatory reaction to circumvent the autophagic defect under Pten-deficiency.

Morphological data obtained by electron microsopy demonstrate that autophagic vacuoles (autophagosomes plus autolysosomes) accumulating in the presence of leupeptin decreased by ~70% in Pten-deficient livers compared with control livers. This marked reduction in the number of autophagic vacuoles is likely due to an impaired autophagosome formation and is considered to be a major cause of the defect in autophagic protein degradation. In addition, we were able to assess the reduction in autophagosome maturation into autolysosome in Pten-deficiency by biochemical techniques. The centrifugal analysis of denser autolysosomes isolated from leupeptin-administered livers clearly showed that the inhibition of autophagosome maturation into autolysosomes contributes significantly to the defects in autophagic proteolysis. Leupeptin-inhibited autolysosomes from control livers were separated at the bottom fractions in Percoll density-gradient centrifugation and possessed lysosomal (β-hexosaminidase and LGP85), autophagosomal (LC3-II), and autolysosomal (p32) markers. The distribution of these marker proteins in favor of the denser fractions was considerably inhibited in the fractions obtained from Pten-deficient livers.

The inactivation and decreased expression of Pten has frequently been observed in many types of cancer cells, including hepatocellular carcinomas, glioblastomas, breast cancers and prostate cancer.[45,46] It has been also noted that autophagy is suppressed in many cancer cells and the inactivation of Pten has been proposed as a potential mechanism for the suppressed autophagy in cancer cells.[17] In summary our data provides the first evidence showing that the loss of Pten function causes a strong inhibition of the formation and subsequent maturation of autophagosomes, but does not affect *ATG* conjugation reactions. In the yeast *Saccharomyces cerevisiae*, all *ATG* gene products cooperate with one another to form the pre-autophagosomal structure in starvation-induced autophagy.[47] The pre-autophagosomal structure consists of an Atg12-Atg5 conjugate and the lipidated form of Atg8 (yeast counterpart of LC3-II) as essential components and is thought to be an organizing center for autophagosomes. For the organization of the pre-autophagosomal structure, the function of the class III PI3-kinase complex together with Atg16 and Atg9 is required. Meanwhile, some Atg proteins, including Atg1 protein kinase (class A Atg proteins), are required for the late stages of autophagosome formation. In other words, they play pivotal roles as a bridge between the pre-autophagosomal structure and autophagosomes.[47] It is possible that the loss of Pten function or hyper activation of class I PI3-kinase/Akt elicits the inhibition of the mammalian counterparts of class A Atg proteins. The identification and characterization of mammalian class A Atg proteins, which awaits future investigation, will be important in developing a better understanding of the mechanism of the autophagy defect in the Pten-deficiency.

Materials and Methods

Control and hepatocyte specific Pten-deficient mice. *Pten$^{flox/flox}$* mice (129Ola x C57BL6/J F2) were mated to *AlbCre* transgenic mice (C57BL6/J) as described previously.[24] The expression of Cre is controlled by the promoter of the hepatocyte-specific *albumin* gene. Offspring carrying *AlbCre* plus two copies of the floxed *Pten* allele (*AlbCrePten$^{flox/flox}$*), *AlbCre* plus one copy of the floxed *Pten* allele (*AlbCrePten$^{Flox/+}$*), and *AlbCre* plus two copies of the wild type *Pten* allele (*AlbCrePten$^{+/+}$*) correspond to homozygous mutant, heterozygous mutant and wild-type mice, respectively. For all experiments described herein, homozygous mutant mice and wild type mice between 10 to 15 weeks after birth were used as Pten-deficient and control mice, respectively. All animal experiments were approved by the Institutional Review Board of the Akita University School of Medicine and the Review Board of the Center for Biomedical Research Resources of Juntendo University.

DNA microarray. RNAs purified from Pten-deficient and control hepatocytes were amplified, converted to complementary DNAs, and labeled with cyanin 3-CTP and cyanin 5-CTP using a LRIFLA kit (Agilent Technologies, Palo Alto, CA) following the manufacturer's recommended protocol. The resulting amplified complementary RNAs were fragmented and hybridized using the Agilent in situ hybridization plus kit (Agilent Technologies) and subjected to DNA microarray analysis as described by Sato et al.[25]

RT-PCR. RT-PCR was performed for the following seven genes: beclin (Atg6), MAP-LC3B, Atg3, Atg7, Atg10, Atg12, Atg16 and β actin. One microgram of RNA samples prepared as templates for the DNA microarray analysis was treated with DNase (Life Technologies, Gaithersburg, MD) and then reverse transcribed using the TaqMan SuperScript™ first strand synthesis system for RT-PCR (Invitrogen, Carlsbad, CA) according to the manufacturer's instructions. RT-PCR was carried out according to the method described previously.[24] The following primer sequences were used: Beclin, forward primer (AGCTCAGTACCAGCGGGAGT) and reverse primer (TGGAAGGTGGCATTGAAGAC); LC3B, forward primer (AGATAATCAGACGGCGCTTG) and reverse primer (ATGTCTCCTGCGAGGCATAA); Atg3, forward primer (ATCCTCATCTCCCACCACCT) and reverse primer (TTGGAATGACAGCTTGAACAAA); Atg7, forward primer (GCTGTGGAGCTGATGGTCTC) and reverse primer (CCAGGCTGACAGGAAGAACA); Atg10, forward primer (CCCAGCAGGAACATCCAATA) and reverse primer (AGGCTCAGCCATGATGTGAT); Atg12, forward primer (AACAAAGAAATGGGCTGTGG) and reverse primer (TTGCAGTAATGCAGGACCAG); Atg16L, forward primer (GAATTCAAGGGCTCCCTGTC) and reverse primer (CCTGTGAGTGTGTGCCGTAA); β actin, forward primer (TCC ATG AAA TAA GTG GTT ACA GGA AGT C) and reverse primer (CAA AAA TGA AGT ATT AAG GCG GAA GAT T). The signal for β actin RNA was used as an internal control. All samples were run in triplicate and the final quantification was archived using a relative standard curve.

Electron microscopy. Mouse livers were perfused and fixed with 3% glutaraldehyde (TAAB Laboratory Equipment Ltd., Reading, UK) in 0.05 M sodium cacodylate buffer at pH 7.2, post-fixed with 2% osmic acid, epon-embedded, sectioned at a thickness of 1 μm, and stained with toluidine blue. Ultrathin sections were observed using a Hitachi H7100 electron microscope.

Protein degradation assay. Primary hepatocytes were isolate from control wild type and mutant mice according to a conventiona collagenase perfusion procedure[26] and cultured in Williams' mediun E containing 10% FCS (Williams E/10% FCS), as described.[2 Hepatocytes grown in 24-well microplates were incubated wit Williams E/10% FCS containing [^{14}C]-leucine (0.5 μCi/ml) fo 22 h to label long-lived proteins. The cells were then washed wit Williams E/10% FCS containing 2 mM unlabelled leucine an incubated with the medium for 2 h to allow degradation of short lived proteins and to minimize the incorporation of labeled leucin released by proteolysis into protein. The cells were then washed wit 20 mM Na-phosphate, pH 7.4, 0.15 M NaCl (PBS) and incubate at 37°C with Krebs-Ringer bicarbonate buffer and Williams E/10% FCS in the presence or absence of protease inhibitors. During th next 4 h of the chase period, aliquots of the medium were taken an a one-tenth volume of 100% trichloroacetic acid was added to eac aliquot. The mixtures were centrifuged at 12,000 x g for 5 minute and acid-soluble radioactivity was determined by liquid scintillatio counting. At the end of the experiment, the cultures were washe with PBS, and 1 ml of cold trichloroacetic acid was added to fix th cell proteins. The fixed-cell monolayers were washed with trichlo roacetic acid and dissolved in 0.5 ml of 1N NaOH at 37°C. Th amount of radioactivity in an aliquot of 1 N NaOH was determine by liquid scintillation counting. Percent protein degradation wa calculated according to a previously published procedure.[28]

Density-shift assay of leupeptin-induced autolysosomes usin percoll gradient centrifugation. Leupeptin (0.4 mg) dissolved i 0.9% NaCl was injected intraperitoneally into control and mutan mice that had been starved for 48 h. The mice were killed after 1 and the livers were excised, dissected into small pieces with scissor and suspended in 4 volumes of ice-cold 5 mM Tes-NaOH, pH 7.4 0.3 M sucrose, 0.5 μg/ml leupeptin, 0.5 μg/ml pepstatin (extractio buffer). The mixture was homogenized with a motor-driven, loos fitting glass/Teflon homogenizer (4 up-down strokes at 800 rpm The homogenate was centrifuged at 500 x *g* for 5 minutes, and th postnuclear supernatant was carefully removed. The precipitate wa suspended in extraction buffer (5 ml/liver) and recentrifuged at 50 x *g* for 5 minutes. The combined postnuclear supernatants wer supplemented with 100 mM $CaCl_2$ to give a final concentration of mM. The resulting suspension was incubated at 30°C for 10 minut to allow the mitochondria to swell, and then it was centrifuged a 12,000 x *g* for 20 minutes. The pelleted mitochondrial/lysosom fraction was suspended in extraction buffer. A portion (2 ml) of th suspension was loaded onto 23 ml of 53% Percoll containing 5 mM Tes-NaOH, pH 7.4, 0.3 M sucrose and centrifuged at 50,000 x g fo 45 minutes using a Beckman 50.2 Ti rotor. After the centrifugation fractions of 1.5 ml were collected from the bottom to the top.

In experiments shown in Figure 2C, mitochondrial/lysosoma microsomal and cytosolic fractions were prepared from starve normal and Pten-deficient livers without leupeptin administration Namely, the post-nuclear supernatants obtained as described abov were centrifuged at 12,000 x *g* for 20 minutes. The pelleted mito chondrial/lysosomal fraction was suspended in extraction buffe The supernatants (post mitochondrial/lysosomal supernatant) wer further centrifuged at 100,000 x *g* for 1 hr. The resultant pelle and supernatants were used as microsomal and cytosolic fraction respectively.

Reagents. Leupeptin, pepstatin and E64d were obtained from the Peptide Institute, Inc., (Osaka, Japan). Percoll was purchased from GE Healthcare Biosceince Co., (Piscataway, NJ). Protein A-Agarose was obtained from Santa Cruz Biotechnology, Inc., (Santa Cruz, CA). Williams medium E was purchased from Invitrogen Corp., (Carlsbad, CA). Fetal calf serum albumin (FCS) was purchased from JRH Biosciences Inc., (Menesas, KS). Paraformaldehyde was obtained from Merck (Darmstadt, Germany). Nonidet P-40 (NP-40) and digitonin were obtained from Nacalai Tesque, Inc., (Kyoto, Japan). [^{14}C]-leucine (300 mCi/mmol) was purchased from Perkin Elmer Co., Ltd. (Boston, MA).

Antibodies. Rabbit antibodies against phosphorylated and unphosphorylated forms of Pten, Akt and ribosomal S6 subunit were obtained from Cell Signaling Technology (Danvers, MA). Horseradish peroxidase-labeled antibodies against rabbit and mouse IgG (heavy and light chains) were purchased from Jackson ImmunoResearch Laboratories, Inc., (West Grove, PA).

To prepare antibodies against Atg12, LC3, beclin and GABARAP, the maltose-binding protein (MalBP) fused with mouse Apg12 (mAtg12), and glutathione-S-transferase (GST) fused with human LC3 (GST-hLC3), human beclin 1 (GST-hbeclin) and human GABARAP (GST-hGABARAP) were overexpressed in *E. coli* grown in a 1 l culture at 37°C for 18 h. The fusion proteins were purified by affinity chromatography on an amylose or glutathione-Sepharose column, and 200 mg of each of the purified fusion proteins was emulsified in complete Freund's adjuvant and injected subcutaneously into Japanese white rabbits. Four, six and eight weeks later, each rabbit was injected with a booster of 100 mg of the appropriate antigen emulsified in incomplete Freund's adjuvant. Antisera were precipitated by ammonium sulfate (50% saturation) and dialyzed against PBS, and the antibodies were affinity-purified by adsorption to MalBP-mAtg12-, GST-hLC3- GST-hbeclin- or GST-hGABARAP-immobilized Sepharose columns, followed by elution with 0.2 M glycine-HCl (pH 2.8). Each eluate was concentrated using an Amicon Diaflo apparatus (Danvers, MA) and passed through a MalBP- or GST-immobilized Sepharose column to remove anti-MalBP and anti-GST antibodies. Antibodies to Atg7 and Atg5 were prepared as described previously.[29,30] An antibody that specifically recognizes a 32 k fragment of betaine homocysteine methyltransferase (BHMT) was prepared according to a previously published procedure.[27] An antibody to initiation factor 4E-binding protein was purchased from Zymed Laboratories, Inc., (South San Francisco, CA).

Biochemical procedures. Protein concentrations were determined using a BCA protein assay following the manufacturer's protocol (Pierce). Sodium dodecyl sulfate (SDS)-polyacrylamide gel electrophoresis was carried out according to a published procedure.[31] Immunoblot analyses were performed as described previously[32] using an ECL Western Blot Detection Kit (Amersham) as the substrate for the horseradish peroxidase conjugate of the second antibodies. Beta-hexosamidase activity was measured as described previously[33] using 4-methyl-umbelliferyl-b-D-glucosaminide as the substrate.

Acknowledgements

This work was supported, in part, by grants-in-aid (Nos. 17025038 and 17028050 to M.K., No. 18390213 to S.W.) for Scientific Research, grant-in-aid (No. 12146205 to E.K.) for Scientific Research on Priority Areas from the Ministry of Education Science, Sports and Culture of Japan, and grant-in-aid for the Third-Term Comprehensive 10-Year Strategy for Cancer Control from the Ministry of Health, Labor and Welfare (No. 16271401 to T.U.) The authors thank Naoko Minematsu and Hideko Uga for technical assistance in the preparation of antibodies.

References

1. Alessi DR, Downes CP. The role of PI 3-kinase in insulin action. Biochim Biophys Acta 1998; 1436:151-64.
2. Accili D, Kido Y, Nakae J, Lauro D, Park BC. Genetics of type 2 diabetes: insight from targeted mouse mutants. Curr Mol Med 2001; 1:9-23.
3. Bevan P. Insulin signalling. J Cell Sci 2001; 114:1429-30.
4. Fruman DA, Meyers RE, Cantley LC. Phosphoinositide kinases. Annu Rev Biochem 1998 67:481-507.
5. Klippel A, Kavanaugh WM, Pot D, Williams LT. A specific product of phosphatidylinositol 3-kinase directly activates the protein kinase Akt through its pleckstrin homology domain Mol Cell Biol 1997; 17:338-44.
6. Batty IH, Hickinson DM, Downes CP. Cross-talk between phospholipase C and phosphoinositide 3-kinase signalling pathways. Biochem Soc Trans 1997; 25:1132-7.
7. Cross DA, Alessi DR, Cohen P, Andjelkovich M, Hemmings BA. Inhibition of glycogen synthase kinase-3 by insulin mediated by protein kinase B. Nature 1995; 378:785-9.
8. Kitamura T, Ogawa W, Sakaue H, Hino Y, Kuroda S, Takata M, Matsumoto M, Maeda T Konishi H, Kikkawa U, Kasuga M. Requirement for activation of the serine-threonine kinase Akt (protein kinase B) in insulin stimulation of protein synthesis but not of glucose transport. Mol Cell Biol 1998; 18:3708-17.
9. Dufner A, Andjelkovic M, Burgering BM, Hemmings BA, Thomas G. Protein kinase B localization and activation differentially affect S6 kinase 1 activity and eukaryotic translation initiation factor 4E-binding protein 1 phosphorylation. Mol Cell Biol 1999; 19:4525-34.
10. Li J, Yen C, Liaw D, Podsypanina K, Bose S, Wang SI, Puc J, Miliaresis C, Rodgers L McCombie R, Bigner SH, Giovanella BC, Ittmann M, Tycko B, Hibshoosh H, Wigler MH Parsons R. PTEN, a putative protein tyrosine phosphatase gene mutated in human brain breast, and prostate cancer. Science 1997; 275:1943-7.
11. Maehama T, Dixon JE. The tumor suppressor, PTEN/MMAC1, dephosphorylates the lipid second messenger, phosphatidylinositol 3,4,5-trisphosphate. J Biol Chem 1998 273:13375-8.
12. Levine, B. Eating oneself and uninvited guests: autophagy-related pathways in cellular defense. Cell 2005; 120:159-62.
13. Mizushima N, Klionsky DJ. Protein turnover via autophagy: implications for metabolism Annu Rev Nutr 2007; 27:19-40.
14. Schworer CM, Shiffer KA, Mortimore GE. Quantitative relationship between autophagy and proteolysis during graded amino acid deprivation in perfused rat liver. J Biol Chem 1981; 256:7652-8.
15. Tanida I, Ueno, T, Kominami E. LC3 conjugation system in mammalian autophagy. Int J Biochem Cell Biol 2004; 36:2503-18.
16. Mizushima N, Yoshimori T, Ohsumi Y. Role of the Apg12 conjugation system in mammalian autophagy. Int J Biochem Cell Biol 2003; 35:553-61.
17. Ogier Denis E, Codogno P. Autophagy: a barrier or an adaptive response to cancer Biochim. Biophys. Acta 2003; 1603:113-28.
18. Petiot A, Ogier Denis E, Blommaart EF, Meijer AJ, Codogno P. Distinct classes of phosphatidylinositol 3'-kinases are involved in signaling pathways that control macroautophagy in HT-29 cells. J Biol Chem 2000; 275:992-8.
19. Arico S, Petiot A, Beauvy C, Dubbelhuis PF, Meijer AJ, Codogno P, Ogier Denis E. The tumor suppressor PTEN positively regulates macroautophagy by inhibiting the phosphatidylinositol 3-kinase/Protein kinase B pathway. J Biol Chem 2001; 276:35243-6.
20. Kihara A, Noda T, Ishihara N, Ohsumi Y. Two distinct Vps34 phosphatidylinositol 3-kinase complexes function in autophagy and carboxypeptidaseY sorting in *Saccharomyces cerevisiae* J Cell Biol 2001; 152:519-30.
21. Kihara A, Kabeya Y, Ohsumi Y, Yoshimori T. Beclin-phosphatidylinositol 3-kinase complex functions at the trans-Golgi network. EMBO Rep 2001; 2:330-5.
22. Zeng X, Overmeyer JH, Maltese WA. Functional specificity of the mammalian Beclin Vps34 PI 3-kinase complex in macroautophagy versus endocytosis and lysosomal enzyme trafficking. J. Cell Sci 2006; 119:259-70.
23. Stiles B, Wang Y, Stahl A, Bassilian S, Lee, WP, Kim YJ, Sherwin R, Devaskar S, Lesche R Magnuson MA, Wu H. Liver-specific deletion of negative regulator Pten results in fatty liver and insulin hypersensitivity. Proc Natl Acad Sci USA 2004; 101:2082-7.
24. Horie Y, Suzuki A, Kataoka E, Sasaki T, Hamada K, Sasaki J, Mizuno K, Hasegawa G Kishimoto H, Iizuka M, Naito M, Enomoto K, Watanabe, S, Mak TW, Nakano T Hepatocyte-specific Pten deficiency results in steatohepatitis and hepatocellular carcinomas J Clin Invest 2004; 113:1774-83.
25. Sato W, Horie Y, Kataoka E, Ohshima S, Dohmen T, Iizuka M, Sasaki J, Sasaki T, Hamada K Kishimoto H, Suzuki A, Watanabe S. Hepatic gene expression in hepatocyte-specific Pten deficient mice showing steatohepatitis without ethanol challenge. Hepatol Res 2006 34:256-65.

26. Tanaka K, Sato M, Tomita Y, Ichihara A. Biochemical studies on liver functions in primary cultured hepatocytes of adult rats. I. Hormonal effects on cell viability and protein synthesis. J Biochem (Tokyo) 1978; 84:937-46.
27. Ueno T, Ishidoh K, Mineki R, Tanida I, Murayama K, Kadowaki M, Kominami E. Autolysosomal membrane-associated betaine homocysteine methyltransferase. Limited degradation fragment of a sequestered cytosolic enzyme monitoring autophagy. J Biol Chem 1999; 274:15222-9.
28. Gronostajski RM, Pardee AB. Protein degradation in 3T3 cells and tumorigenic transformed 3T3 cells. J Cell Physiol 1984; 119:127-32.
29. Tanida I, Tanida-Miyake E, Ueno T, Kominami E. The human homolog of *Saccharomyces cerevisiae* Apg7p is a protein-activating enzyme for multiple substrates including human Apg12p, GATE-16, GABARAP, and MAP-LC3. J Biol Chem 2001; 276:1701-6.
30. Tanida I, Nishitani T, Nemoto T, Ueno T, Kominami E. Mammalian Apg12p, but not the Apg12p.Apg5p conjugate, facilitates LC3 processing. Biochem Biophys Res Commun 2002; 296:1164-70.
31. Laemmli UK. Cleavage of structural proteins during the assembly of the head of bacteriophage T4. Nature 1970; 227:680-5.
32. Towbin H, Staehelin T, Gordon J. Electrophoretic transfer of proteins from polyacrylamide gels to nitrocellulose sheets: procedure and some applications. Proc Natl Acad Sci USA 1979; 76:4350-4.
33. Lusis AJ, Tomino S, Paigen K. Isolation, characterization, and radioimmunoassay of murine egasyn, a protein stabilizing glucuronidase membrane binding. J Biol Chem 1976; 251:7753-60.
34. Komatsu, M, Waguri S, Ueno T, Iwata J, Murata S, Tanida I, Ezaki J, Mizushima N, Ohsumi Y, Uchiyama Y, Kominami E, Tanaka K, Chiba T. Impairment of starvation-induced and constitutive autophagy in Atg7-deficient mice. J Cell Biol 2005; 169:425-34.
35. Ishikawa T, Furuno K, Kato K. Ultrastructural studies on autolysosomes in rat hepatocytes after leupeptin treatment. Exp Cell Res 1983; 144:15-24.
36. Masaki R, Yamamoto A, Tashiro Y. Cytochrome P-450 and NADPH-cytochrome P-450 reductase are degraded in the autolysosomes in rat liver. J Cell Biol 1987; 104:1207-15.
37. Akagi S, Yamamoto A, Yoshimori T, Masaki R, Ogawa R and Tashiro Y. Distribution of protein disulfide isomerase in rat hepatocytes. J Histochem Cytochem 1988; 36:1533-42.
38. Furuno K, Ishikawa T, Kato K. Appearance of autolysosomes in rat liver after leupeptin treatment. J Biochem (Tokyo) 1982; 91:1485-94.
39. Furuno K, Ishikawa T, Kato K. Isolation and characterization of autolysosomes which appeared in rat liver after leupeptin treatment. J Biochem (Tokyo) 1982; 91:1943-50.
40. Kominami E, Hashida S, Khairallah EA, Katunuma N. Sequestration of cytoplasmic enzymes in an autophagic vacuole-lysosomal system induced by injection of leupeptin. J Biol Chem 1983; 258:6093-100.
41. Ueno T, Muno D, Kominami E. Membrane markers of endoplasmic reticulum preserved in autophagic vacuolar membranes isolated from leupeptin-administered rat liver. J Biol Chem 1991; 266:18995-9.
42. Mammucari C, Milan G, Romanello V, Masiero E, Rudolf R, Del Piccolo P, Burden SJ, Di Lisi R, Sandri C, Zhao J, Goldberg AL, Schiaffino S, Sandri M. FoxO3 controls autophagy in skeletal muscle in vivo. Cell Metab 2007; 6:458-71.
43. Zhao J, Brault JJ, Schild A, Cao P, Sandri M, Schiaffino S, Lecker SH, Goldberg AL. FoxO3 coordinately activates protein degradation by the autophagic/lysosomal and proteasomal pathways in atrophying muscle cells. Cell Metab 2007; 6:472-83.
44. Gohla A, Klement K, Piekorz RP, Pexa K, vom Dahl S, Spicher K, Dreval V, Häussinger D, Birnbaumer L, Nürnberg B. An obligatory requirement for the heterotrimeric G protein G_{i3} in the antiautophagic action of insulin in the liver. Proc Natl Acad Sci USA 2007; 104:3003-8.
45. Hu TH, Huang CC, Lin PR, Chang HW, Ger LP, Lin YW, Changchien CS, Lee CM, Tai MH. Expression and prognostic role of tumor suppressor gene PTEN/MMAC1/TEP1 in hepatocellular carcinoma. Cancer 2003; 97:1929-40.
46. Di Cristofano A, Pandolfi PP. The multiple roles of PTEN in tumor suppression. Cell 2000; 100:387-90.
47. Suzuki K, Kirisako T, Kamada Y, Mizushima N, Noda T, Ohsumi Y. The pre-autophagosomal structure organized by concerted functions of APG genes is essential for autophagosome formation. EMBO J 2001; 20:5971-81.